Supporting Information

Heavier Bis(*m*-terphenyl)element phosphaethynolates of Group 13

Daniel Duvinage,[a] Marvin Janssen,[a] Enno Lork,[a] Hansjörg Grützmacher,[b] Stefan Mebs,*[c]

Jens Beckmann*[a]

[a] *Institut für Anorganische Chemie und Kristallographie, Universität Bremen,*

Leobener Straße 7, 28359 Bremen, Germany

[b] *Department of Chemistry and Applied Biosciences, ETH Zürich, Vladimir-Prelog Weg 1,*

Hönggerberg, 8093 Zürich, Switzerland.

[c] *Institut für Experimentalphysik, Freie Universität Berlin, Arnimallee 14, 14195 Berlin, Germany*

* Correspondence to Jens Beckmann (E-mail: j.beckmann@uni-bremen.de) and Stefan Mebs (E-mail: stefan.mebs@fu-berlin.de)

Table of Contents

Experimental procedures **3**

General information 3

Synthesis of (2,6-$Mes_2C_6H_3$)$_2$GaPCO (1) 4

Synthesis and characterization of (2,6-$Mes_2C_6H_3$)$_2$InPCO (2) 8

Synthesis and characterization of ($Mes_2C_6H_3$)$_2$GaP(O)C(IMe_4) (3) 12

Synthesis and characterization of ($Mes_2C_6H_3$)$_2$InP(O)C(IMe_4) (4) 16

Synthesis and characterization of (2,6-$Mes_2C_6H_3$)$_2$GaTeP(O)C(IMe_4) (5) 20

Synthesis and characterization of (2,6-$Mes_2C_6H_3$)$_2$InTeP(O)C(IMe_4) (6) 27

X-Ray diffraction studies **34**

Computational methodology **37**

References **43**

Experimental procedures

General information

Unless otherwise stated, all reactions and manipulations were performed under inert atmosphere (argon) using anhydrous solvents. The starting materials $(2,6\text{-}Mes_2C_6H_3)_2GaCl$,[S1] $(2,6\text{-}Mes_2C_6H_3)_2InBr$,[S2] $[Na(1,4\text{-dioxane})_{2.5}][PCO]$[S3] and 1,2,3,4-tetramethylimidazol-2-ylidene, IMe_4,[S4] were prepared following the published procedures. Anhydrous dichloromethane, hexane, tetrahydrofuran and toluene were collected from an SPS800 mBraun solvent purification system and stored over 4 Å molecular sieves. Dimethoxyethane was dried over CaH_2 and distilled over 4 Å molecular sieves for storage. Deuterated solvents were degassed and dried over 4 Å molecular sieves under argon.

NMR spectra were recorded at room temperature on a Bruker Avance 600 MHz spectrometer. ^1H, $^{13}C\{^1H\}$, $^{31}P\{^1H\}$ and ^{125}Te NMR spectra are reported on the δ scale (ppm) and are referenced against $SiMe_4$, H_3PO_4 (85% in water) and Me_2Te (90% in C_6D_6). ^1H and $^{13}C\{^1H\}$ chemical shifts are calibrated to the residual peak of the solvent ($CDHCl_2$ 5.32 ppm for CD_2Cl_2; C_6D_5H 7.16 ppm for C_6D_6 and C_4HD_7O: 1.71 ppm for THF-d_8) in the ^1H NMR spectra, and to the peak of the deuterated solvent (CD_2Cl_2 53.84 ppm, C_6D_6 128.06 ppm and THF-d_8: 67.21 ppm) in the $^{13}C\{^1H\}$ NMR spectra. The assignment of the ^1H and $^{13}C\{^1H\}$ resonance signals was made in accordance with the COSY, HSQC and HMBC spectra. The ESI HRMS spectra were measured on a Bruker Impact II spectrometer. Acetonitrile or toluene/acetonitrile solutions ($c = 1\cdot10^{-5}$ mol·L^{-1}) were injected directly into the spectrometer at a flow rate of 3 μL·min^{-1}. Nitrogen was used both as a drying gas and for nebulization with flow rates of approximately 5 L·min^{-1} and a pressure of 5 psi. Pressure in the mass analyzer region was usually about $1\cdot10^{-5}$ mbar. Spectra were collected for 1 min and averaged. The nozzle-skimmer voltage was adjusted individually for each measurement. IR spectra were recorded on a *Nicolet* Thermo iS10 scientific spectrometer with a diamond ATR unit. The absorption bands are reported in cm^{-1} with indicated relative intensities: s (strong, 0 – 33 % T); m (medium, 34 – 66 % T), w (weak, 67 – 100 % T), and br (broad).

Synthesis of (2,6-$Mes_2C_6H_3)_2GaPCO$ (1)

(2,6-$Mes_2C_6H_3)_2GaCl$ (50.0 mg, 68.3 µmol, 1.00 eq.) and [$Na(1,4\text{-dioxane})_{2.5}$][PCO] (17.3 mg, 68.3 µmol, 1.00 eq.) were suspended in toluene (6 mL) and stirred for 18 hours. The suspension has been filtered and the solvent of the remaining solution has been removed under reduced pressure to yield **1** as yellow solid (43 mg, 56.9 µmol, 82%).

^{1}H-NMR (601 MHz, C_6D_6): δ (ppm) = 7.02 (t, $^3J(^1H\text{-}^1H)$ = 7.58 Hz, 1H, H4), 6.84 (s, 4H, H9 and H11), 6.68 (d,$^3J(^1H\text{-}^1H)$ = 7.60 Hz, 2H, H3 and H5), 2.25 (s, 6H, H14), 1.89 (s,12H, H13 and H15). **^{13}C{^{1}H}-NMR** (151 MHz, C_6D_6): δ (ppm) = 186.50 (d,$^1J(^{31}P\text{-}^{13}C)$ = 99.82 Hz, C16), 150.72 (d,$^2J(^{31}P\text{-}^{13}C)$ = 10.53 Hz, C1), 148.18 (s, C2 and C6), 141.46 (s, C7), 137.51 (s, C8 and C12), 137.11 (s, C10), 130.18 (s, C4), 129.51 (s, C3, C5, C9 and C11), 21.96 (s, C13 or C15), 21.94 (s, C13 or C15), 21.28 (s, C14).). **^{31}P{^{1}H}-NMR** (243 MHz, C_6D_6): δ (ppm) = –283.29 (s). **HRMS ESI (**m/z): $[M\text{-}PCO]^+$ calculated. for $C_{48}H_{50}Ga$, 695.31628; found, 695.31476. **IR** (ATR, neat): $\tilde{\nu}$= 2950 (w), 2914 (m), 1898 (s), 1610 (m), 1559 (w), 1482 (w), 1440 (s), 1374 (m), 1261 (w), 1176 (w), 1112 (w), 1081 (w), 1031 (m), 844 (s), 804 (s), 771 (w), 739 (s), 706 (w) cm^{-1}.

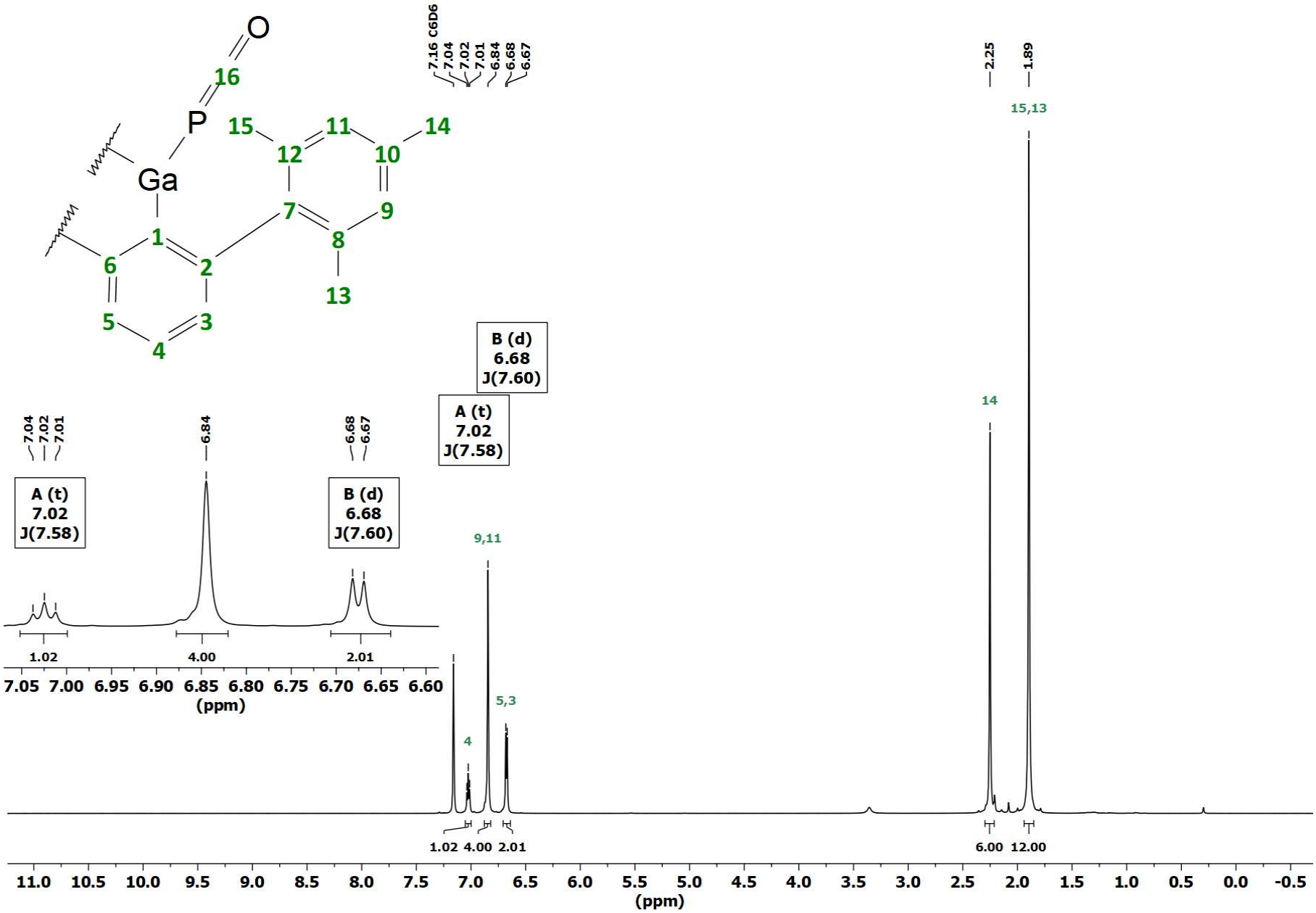

Figure S1. ^{1}H NMR (C_6D_6, 600 MHz) spectrum of (2,6-$Mes_2C_6H_3$)$_2$GaPCO (**1**).

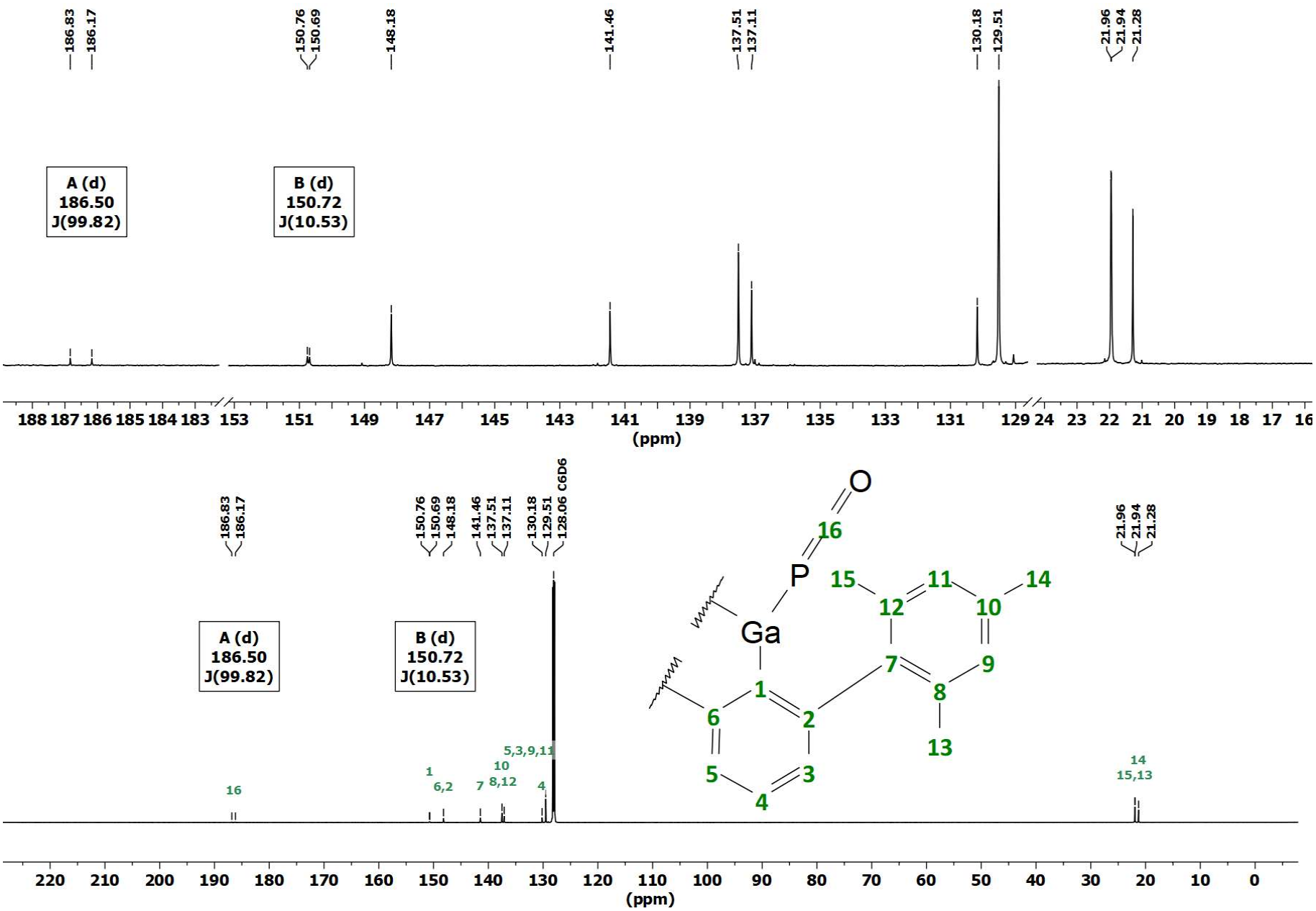

Figure S2. $^{13}C\{^{1}H\}$ NMR (C_6D_6, 151 MHz) spectrum of (2,6-$Mes_2C_6H_3$)$_2$GaPCO (**1**).

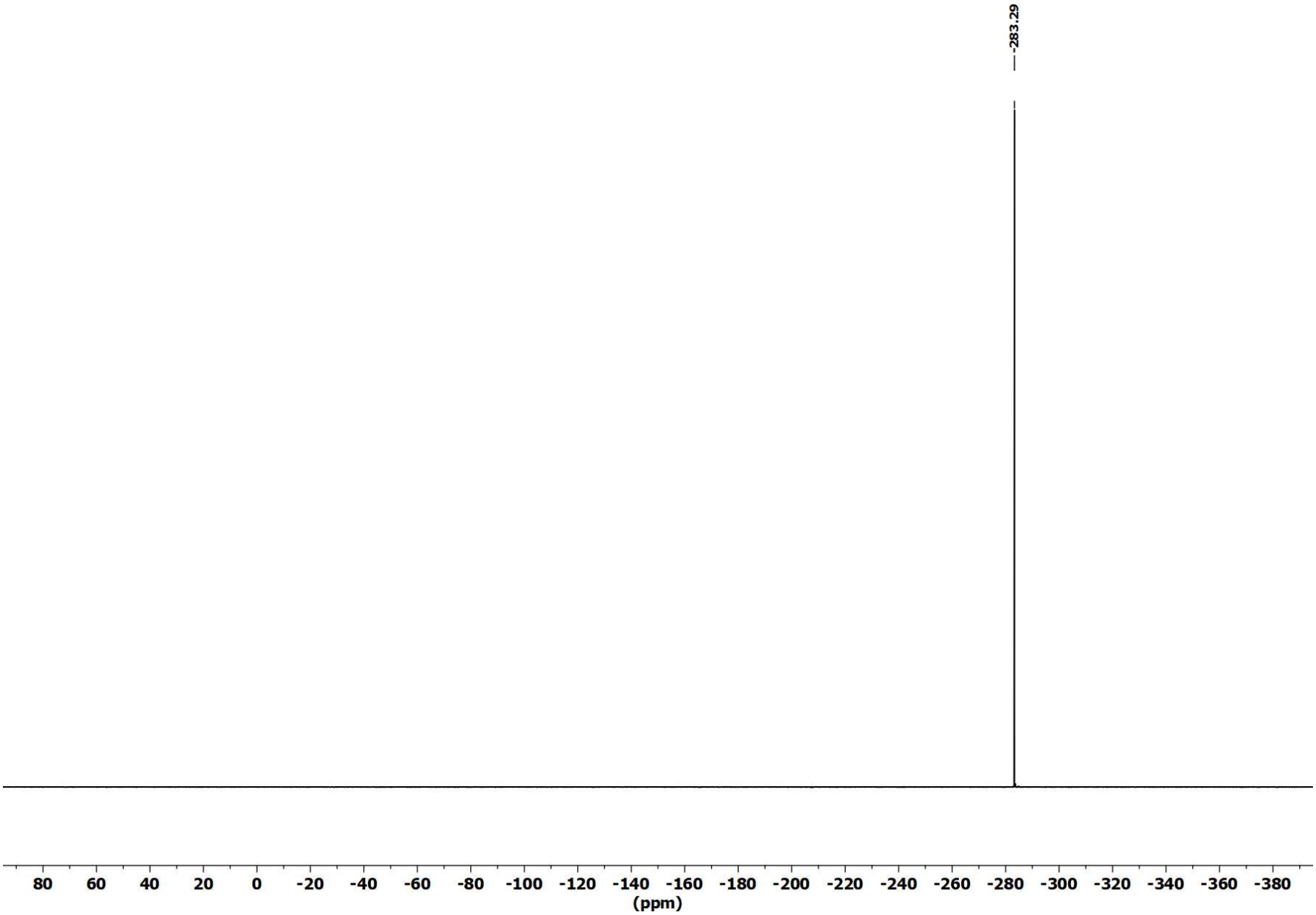

Figure S3. ^{31}P NMR (C_6D_6, 243 MHz) spectrum of (2,6-$Mes_2C_6H_3$)$_2$GaPCO (**1**)

Synthesis and characterization of (2,6-$Mes_2C_6H_3)_2$InPCO (2)

(2,6-$Mes_2C_6H_3)_2$InBr (50.0 mg, 57.4 µmol, 1.00 eq.) and [Na(1,4-dioxane)$_{2.5}$][PCO] (17.3 mg, 57.4 µmol, 1.00 eq.) were suspended in toluene (6 mL) and stirred for 18 hours. The suspension is filtered and the solvent of the remaining solution has been removed under vacuum to yield **2** as yellow solid (40.3 mg, 50.3 µmol, 83%).

^{1}H-NMR (600 MHz, C_6D_6): δ (ppm) = 7.08 (t, ^3J(^{1}H-^{1}H) = 7.54 Hz, 1H, H4), 6.87 (s, 4H, H9 and H11), 6.77 (d,^3J(^{1}H-^{1}H) = 7.53 Hz, 2H, H3 and H5), 2.24 (s, 6H, H14), 1.91 (s, 12H, H13 and H15). **^{13}C{^{1}H}-NMR** (151 MHz, C_6D_6): δ (ppm) = 182.65 (d,^{1}J(^{31}P-^{13}C) = 96.12 Hz, C16), 158.96 (d, ^{1}J(^{31}P-^{13}C) = 9.35 Hz, C1), 148.74 (s, C2 and C6), 141.88 (s, C7), 137.38 (s, C10), 137.24 (s, C8 and C12), 129.65 (s, C4), 129.60 (s, C9 and C11), 128.95 (s, C3 and C5), 21.65 (s, C13 and C15), 21.28 (s, C14). **^{31}P{^{1}H} NMR** (C_6D_6, 243 MHz): δ (ppm) = –336.19 (s). **HRMS ESI** (m/z): $[M\text{-}PCO]^+$ calculated. for $C_{48}H_{50}In$, 741.29458; found, 741.29441. **IR** (ATR, neat): $\tilde{\nu}$= 2914 (m), 1880 (s), 1610 (w), 1564 (w), 1482 (w), 1441 (m), 1374 (w), 1261 (w), 1221 (w), 1175 (w), 1083 (w), 1030 (w), 1012 (w), 879 (w), 846 (s), 801 (s), 774 (w), 746 (w), 735 (s), 699 (w) cm^{-1}.

.

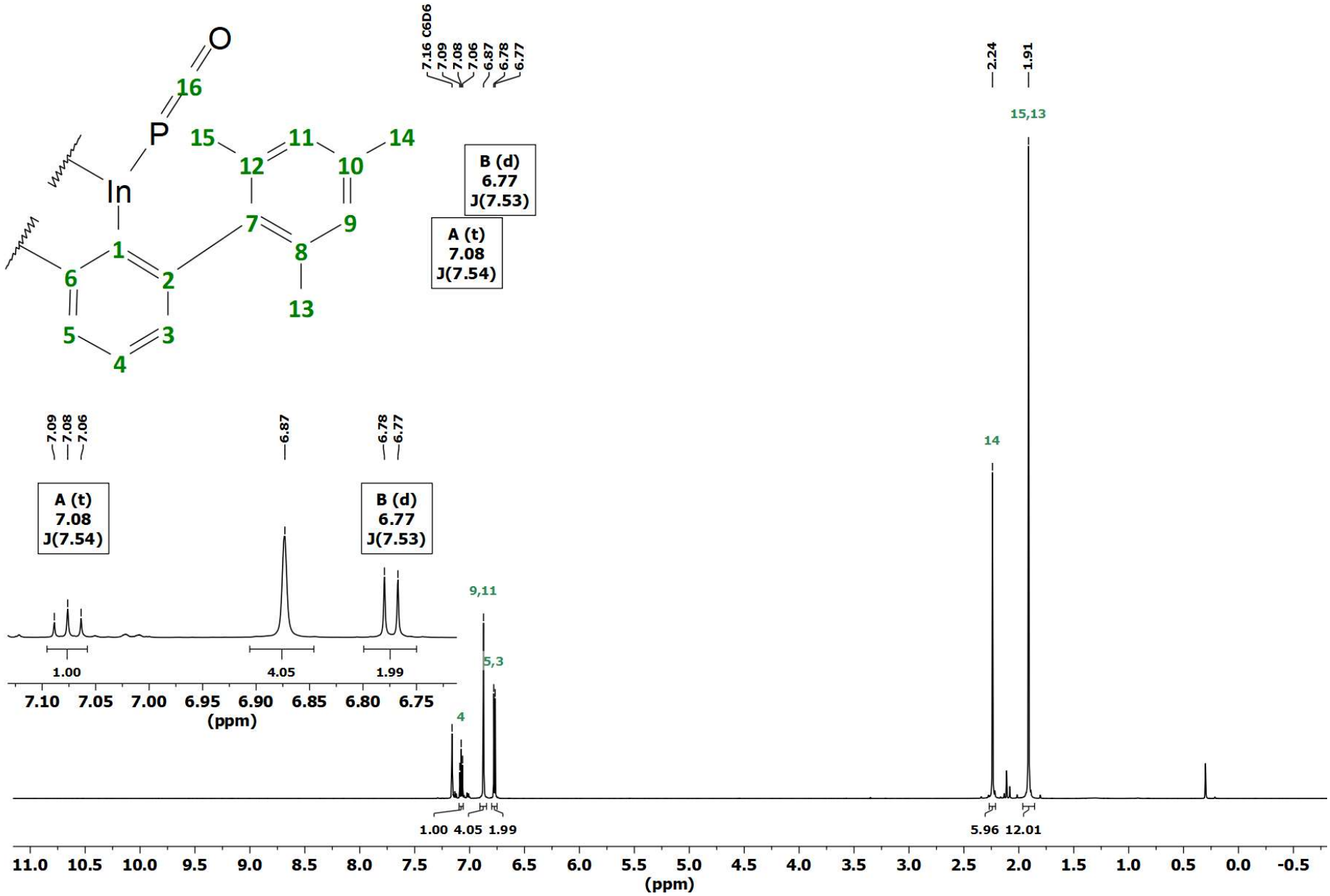

Figure S4. ^{1}H NMR (C_6D_6, 600 MHz) spectrum of (2,6-$Mes_2C_6H_3$)$_2$InPCO (**2**).

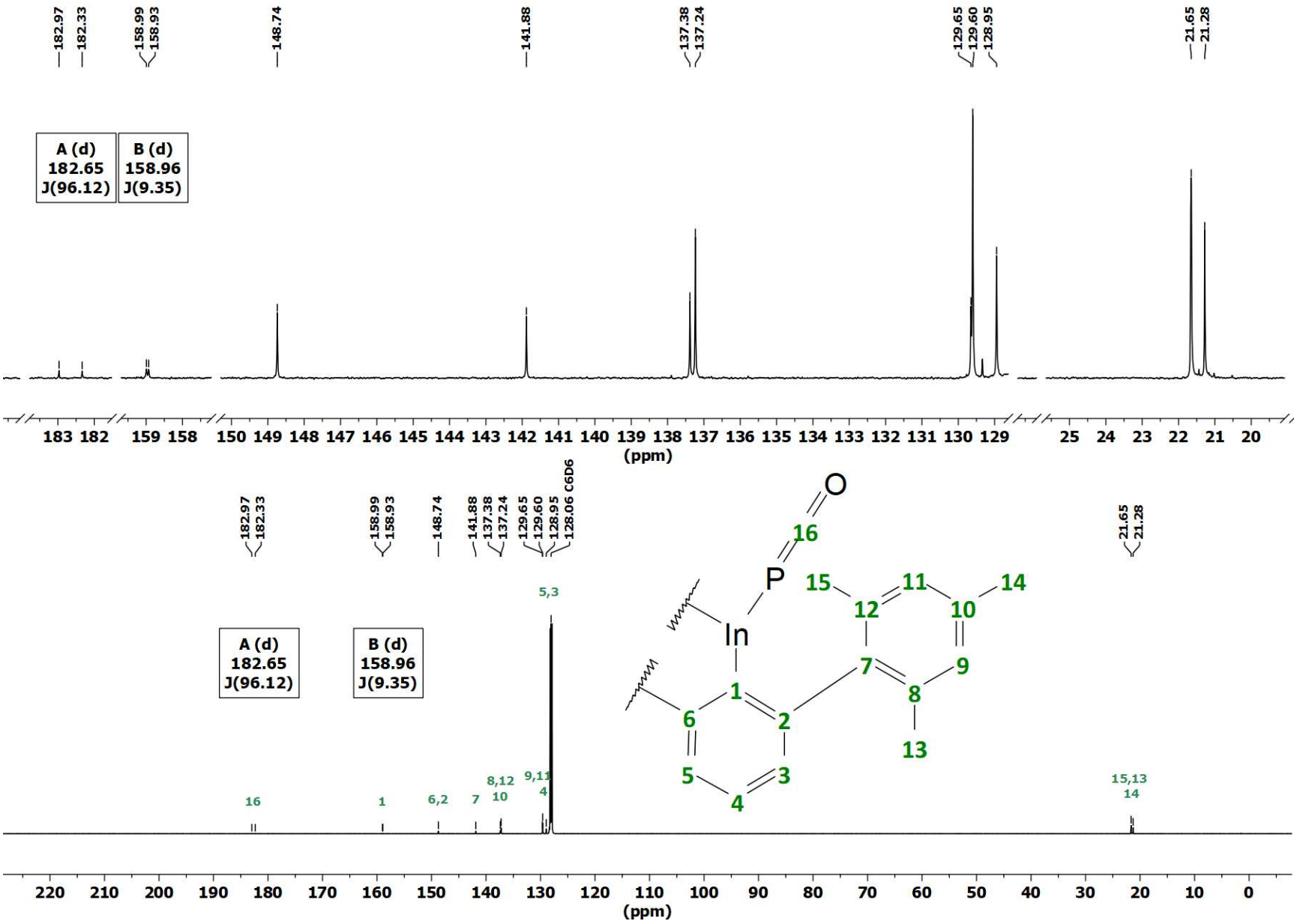

Figure S5. $^{13}C\{^{1}H\}$ NMR (C_6D_6, 151 MHz) spectrum of (2,6-$Mes_2C_6H_3$)$_2$InPCO (**2**).

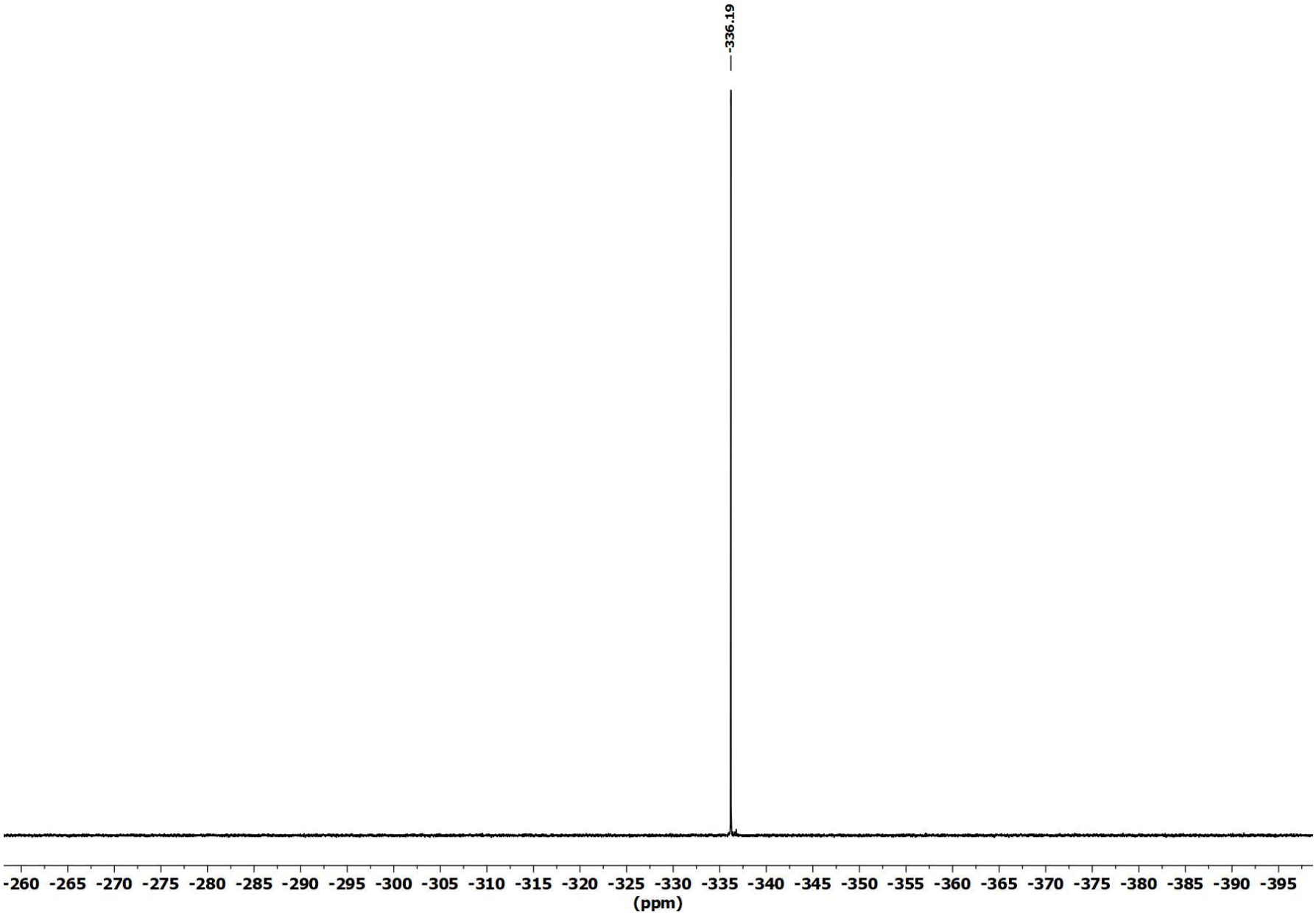

Figure S6. ^{31}P NMR (C_6D_6, 243 MHz) spectrum of (2,6-$Mes_2C_6H_3$)$_2$InPCO (**2**).

Synthesis and characterization of $(Mes_2C_6H_3)_2GaP(O)C(IMe_4)$ (3)

1 (50.0 mg, 66.2 µmol, 1.00 eq.) and 1,3,4,5-tetramethylimidazol-2-ylidene (8.35 mg, 66.2 µmol, 1.00 eq.) were dissolved in toluene (6 mL) and stirred for 4 hours. Afterwards the solution has been filtered through a PTFE syringe filter and the solvent has been removed under vacuum to yield **3** as yellow solid (45.0 mg, 48.6 µmol, 73%).

^{1}H-NMR (600 MHz, CD_2Cl_2): δ (ppm) = 7.06 (t, $^3J(^1H\text{-}^1H)$ = 7.50 Hz, 1H, H4), 6.64 (s (br), 2H, H9 or H11), 6.61 (s (br), 2H, H9 or H11), 6.51 (d, $^3J(^1H\text{-}^1H)$ = 7.46 Hz, 2H, H3 and H5), 3.65 (s, 3H, H20 and H23), 2.19 (s, 6H, H14), 2.15 (s, 3H, H21 and H22), 1.69 (s (br), 6H, H13 or H15), 1.67 (s (br), 6H, H13 or H15). **^{13}C{^{1}H}-NMR** (151 MHz, CD_2Cl_2): δ (ppm) = 196.20 (d, $^1J(^{31}P\text{-}^{13}C)$ = 73.74 Hz, C16), 153.40 (d, $^2J(^{31}P\text{-}^{13}C)$ = 4.14 Hz, C1), 149.63 (s, C2 and C6), 144.48 (s, C7), 141.96 (d, $^2J(^{31}P\text{-}^{13}C)$ = 17.41 Hz, C17), 137.53 (s, C8 or C12), 137.38 (s, C8 or C12), 135.22 (s, C10), 128.65 (s, C3 and C5), 128.32 (s, C9 or C11), 127.90 (s, C9 or C11), 126.55 (s, C4), 124.36 (s, C18 and C19), 34.93 (s, C20 or C23), 34.85 (s, C20 or C23), 22.77 (s, C13 or C15), 22.67 (s, C13 or C15), 21.25 (s, C14), 9.27 (s, C21 and C22). **^{31}P{1H}-NMR** (243 MHz, CD_2Cl_2): δ (ppm) = 245.41 (s). **HRMS ESI** (m/z): [M-PCO-NHC]$^+$ calculated. for $C_{48}H_{50}Ga$, 695.31628; found, 695.31588. **IR** (ATR, neat): $\tilde{\nu}$= 2949 (w), 2912 (m), 2842 (w), 1647 (w), 1609 (w), 1558 (w), 1480 (m), 1433 (s), 1372 (m), 1238 (w), 1215 (s), 1178 (w), 1116 (w), 1073 (w), 1030 (m), 1015 (m), 845 (s), 802 (s), 765 (w), 736 (s), 710 (w), 697 (m), 666 (w) cm^{-1}.

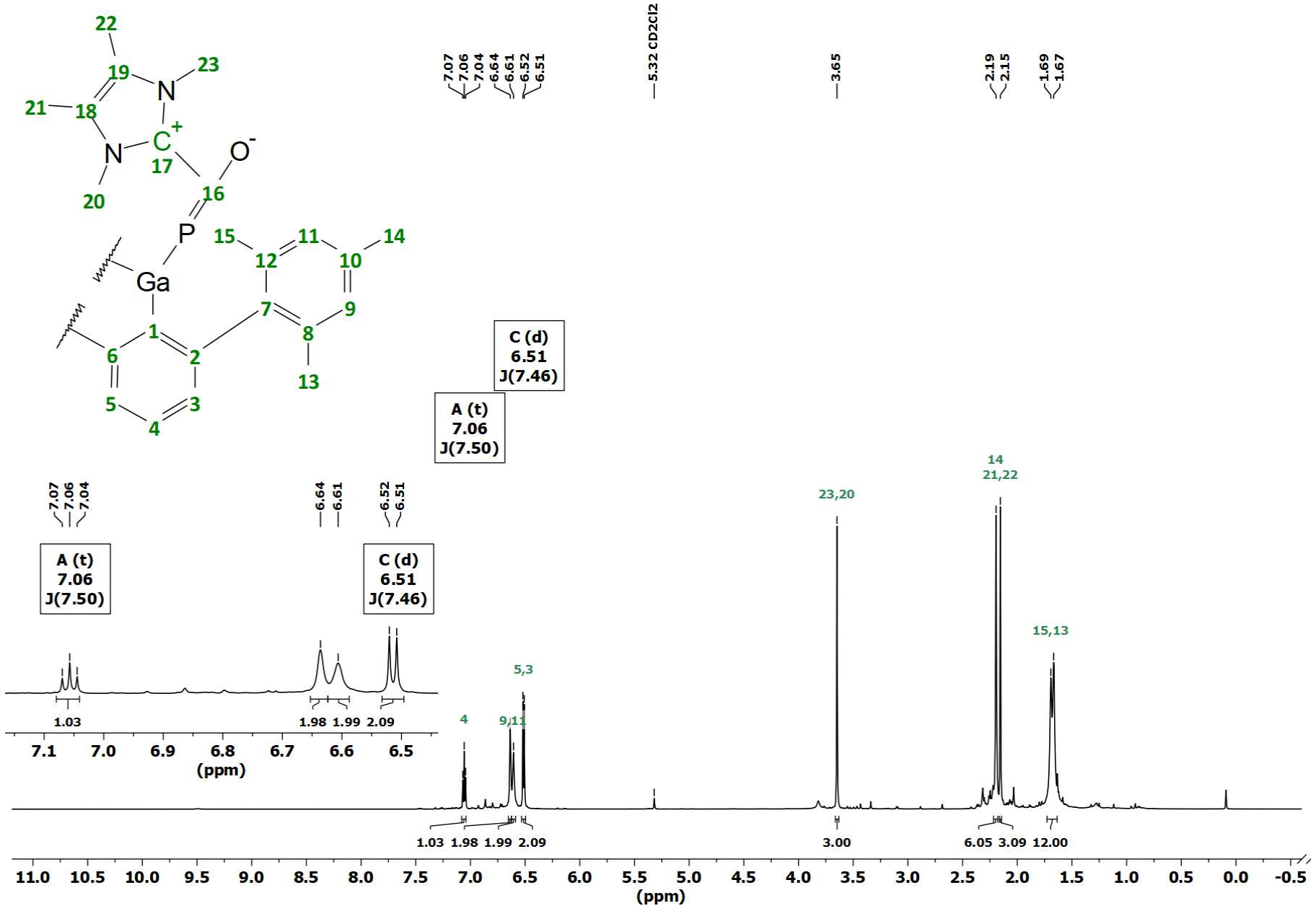

Figure S7. ^{1}H NMR (CD_2Cl_2, 600 MHz) spectrum of (2,6-$Mes_2C_6H_3$)$_2$GaP(O)C(IMe_4) (**3**).

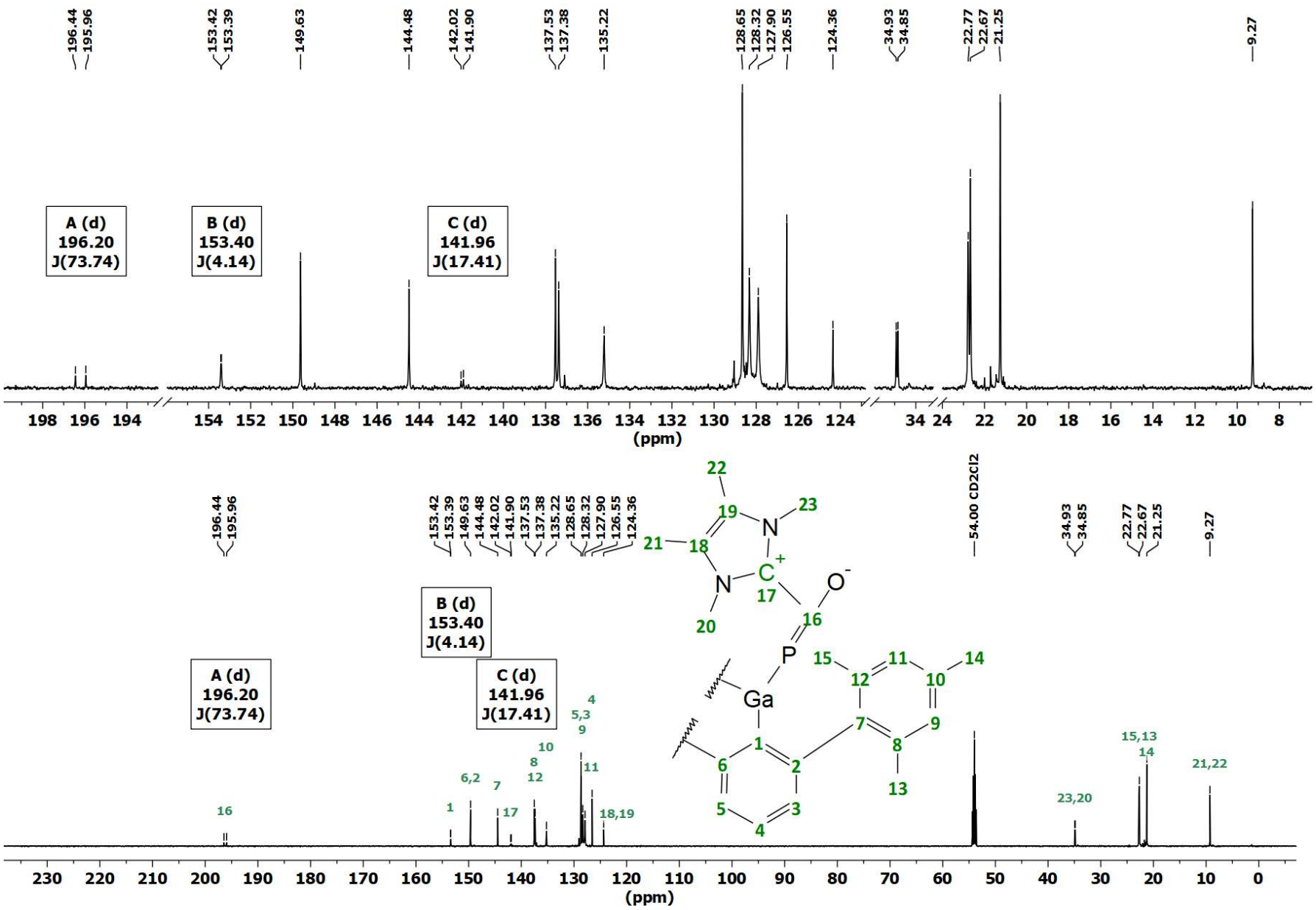

Figure S8. $^{13}C\{^{1}H\}$ NMR (CD_2Cl_2, 151 MHz) spectrum of (2,6-$Mes_2C_6H_3$)$_2$GaP(O)C(IMe_4) (**3**).

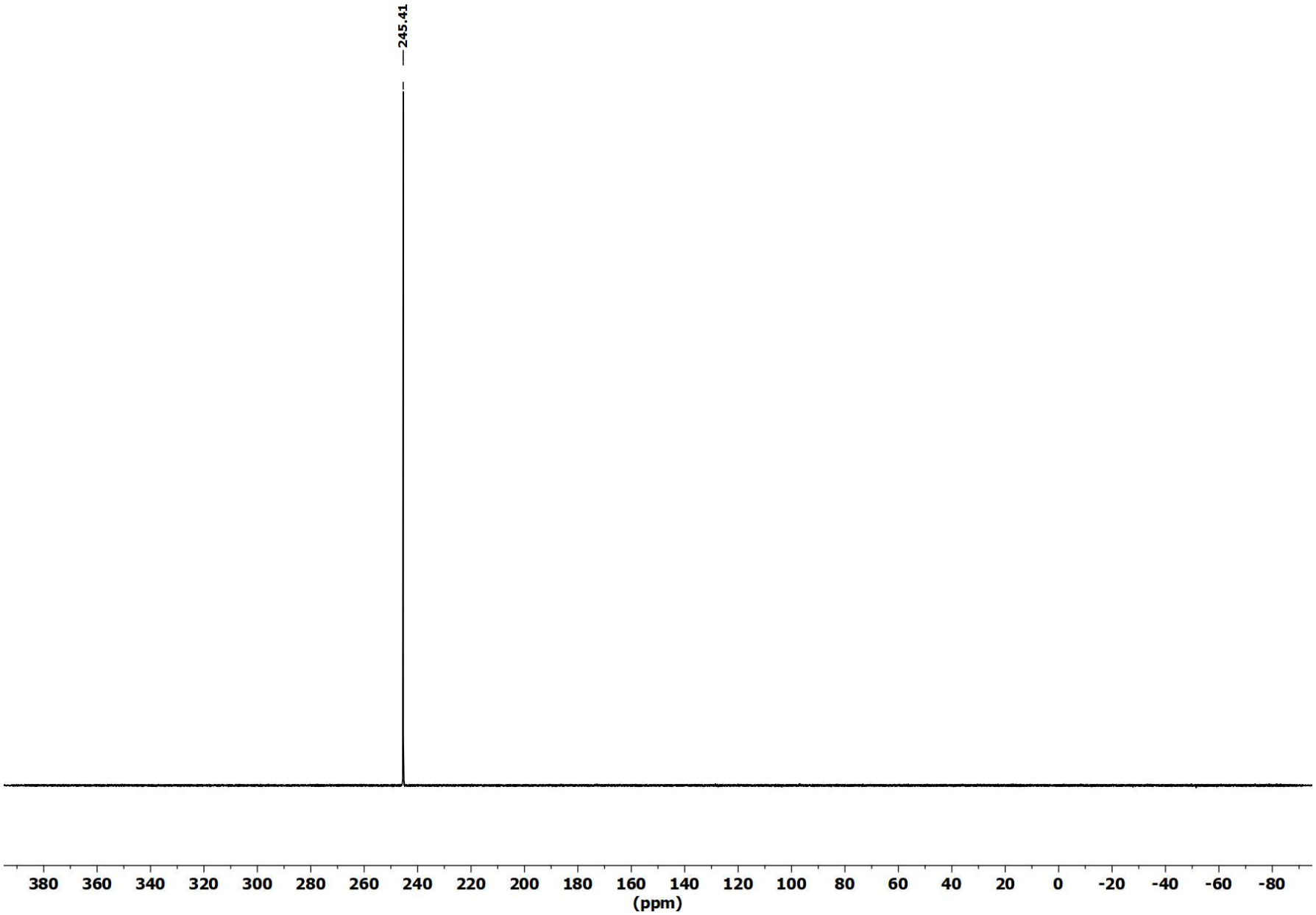

Figure S9. ^{31}P NMR (CD_2Cl_2, 243 MHz) spectrum of (2,6-$Mes_2C_6H_3$)$_2$GaP(O)C(IMe_4) (**3**).

Synthesis and characterization of $(Mes_2C_6H_3)_2InP(O)C(IMe_4)$ (4)

2 (50.0 mg, 62.4 µmol, 1.00 eq.) and 1,3,4,5-tetramethylimidazol-2-ylidene (7.75 mg, 62.4 µmol, 1.00 eq.) were dissolved in toluene (6 mL) and stirred for 4 hours. The solution has been filtered with a PTFE syringe filter and the remaining solvent has been removed under reduced pressure to yield **4** as yellow solid (41.2 mg, 44.5 µmol, 71%).

^{1}H-NMR (600MHz, THF-d_8): δ(ppm) = 7.01 (t,^3J(^{1}H-^{1}H) = 7.48 Hz, 1H, H4), 6.66 (s (br), 2H, H9 or H11), 6.62 (s (br), 2H, H9 or H11), 6,55 (d,^3J(^{1}H-^{1}H) = 7.49 Hz, 2H, H3 and H5), 3.70 (s,3H, H20 and H23), 2.19 (s, 3H, H21 and H22), 2.17 (s, 6H, H14), 1.75 (s, 6H, H13 or H15), 1.72 (s, 6H, H13 or H15). **^{13}C{^{1}H}-NMR** (151 MHz, THF-d_8): δ(ppm) = 198.68 (d,^1J(^{31}P-^{13}C) = 79.69 Hz, C16), 161.98 (s, C1), 150.56 (s, C2 and C6), 145.55 (d,^2J(^{31}P-^{13}C) = 24.36 Hz, C17), 145.05 (s,C7), 137.32 (s, C8 or C12), 137.28 (s, C8 or C12), 135.41 (s, C10), 129.16 (s, C9), 128.60 (s, C11), 128.19 (s, C3 and C5), 127.06 (s, C4), 124.58 (s, C18 and C19), 34.93 (s,C20 or C23), 34.85 (s, C20 or C23), 22.83 (s, C13 or C15), 21.47 (s, C14), 8.62 (s, C21 and C22). **^{31}P{^{1}H}-NMR** (243MHz,THF-d_8): δ(ppm) = 219.65 (s). **HRMS ESI** (m/z): $[M\text{-}PCO\text{-}NHC]^+$ calculated. for $C_{48}H_{50}In$, 741.29458; found, 741.29282, $[M\text{-}PCO]^+$ calculated. for $C_{55}H_{62}InN_2$, 865.39463; found, 865.39352. **IR** (ATR, neat): $\tilde{\nu}$= 2913 (s), 2853 (m), 1770 (w) 1648 (w), 1610 (w), 1558 (w), 1481 (m), 1436 (s), 1372 (m), 1249 (s), 1222 (m), 1177 (w), 1078 (w), 1030 (m), 1008 (m), 952 (w), 845 (s), 800 (s), 768 (w), 734 (s), 712 (m), 697 (m) cm^{-1}.

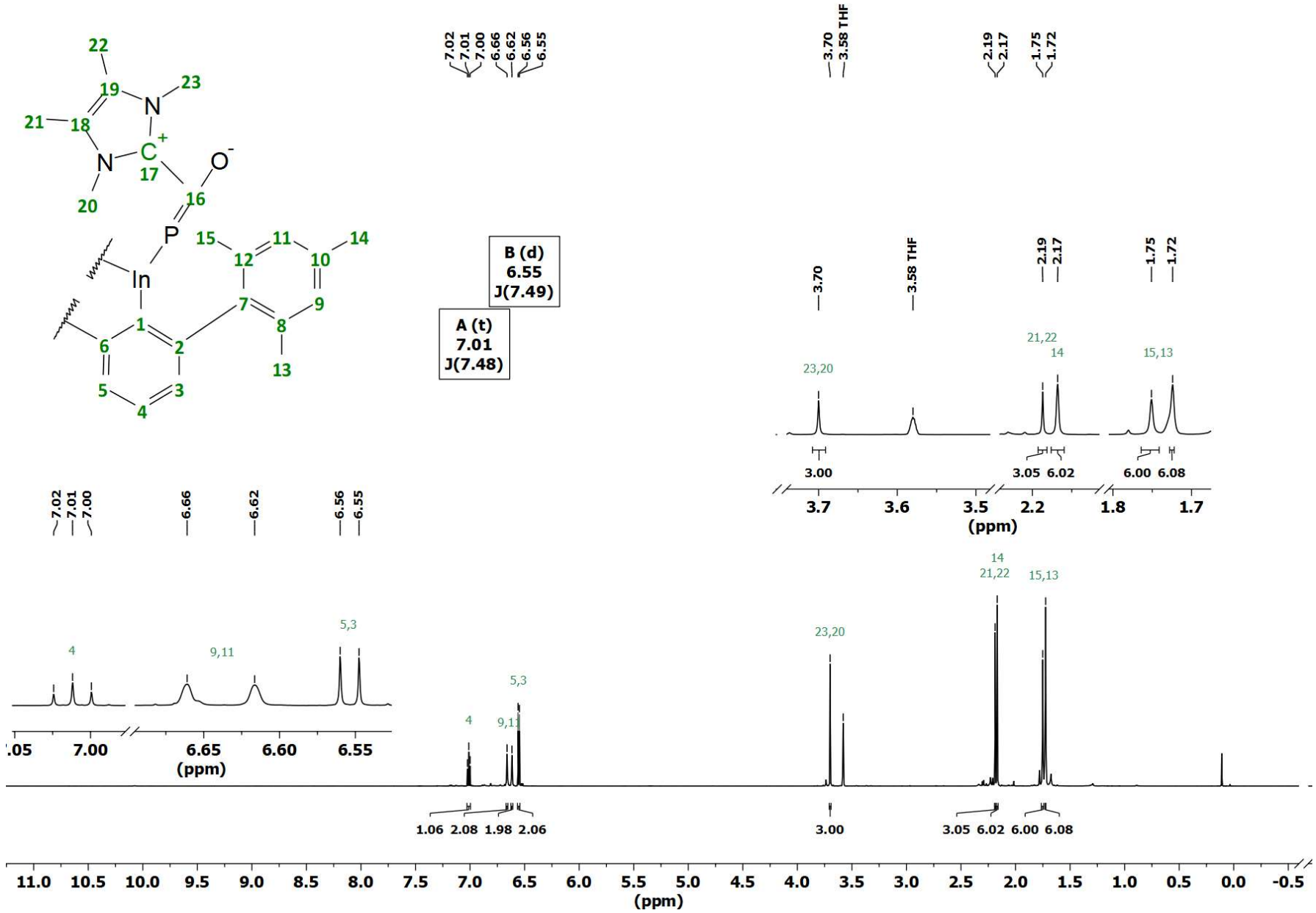

Figure S10. ^{1}H NMR (C_6D_6, 600 MHz) spectrum of (2,6-$Mes_2C_6H_3$)$_2$InP(O)C(IMe_4) (**4**).

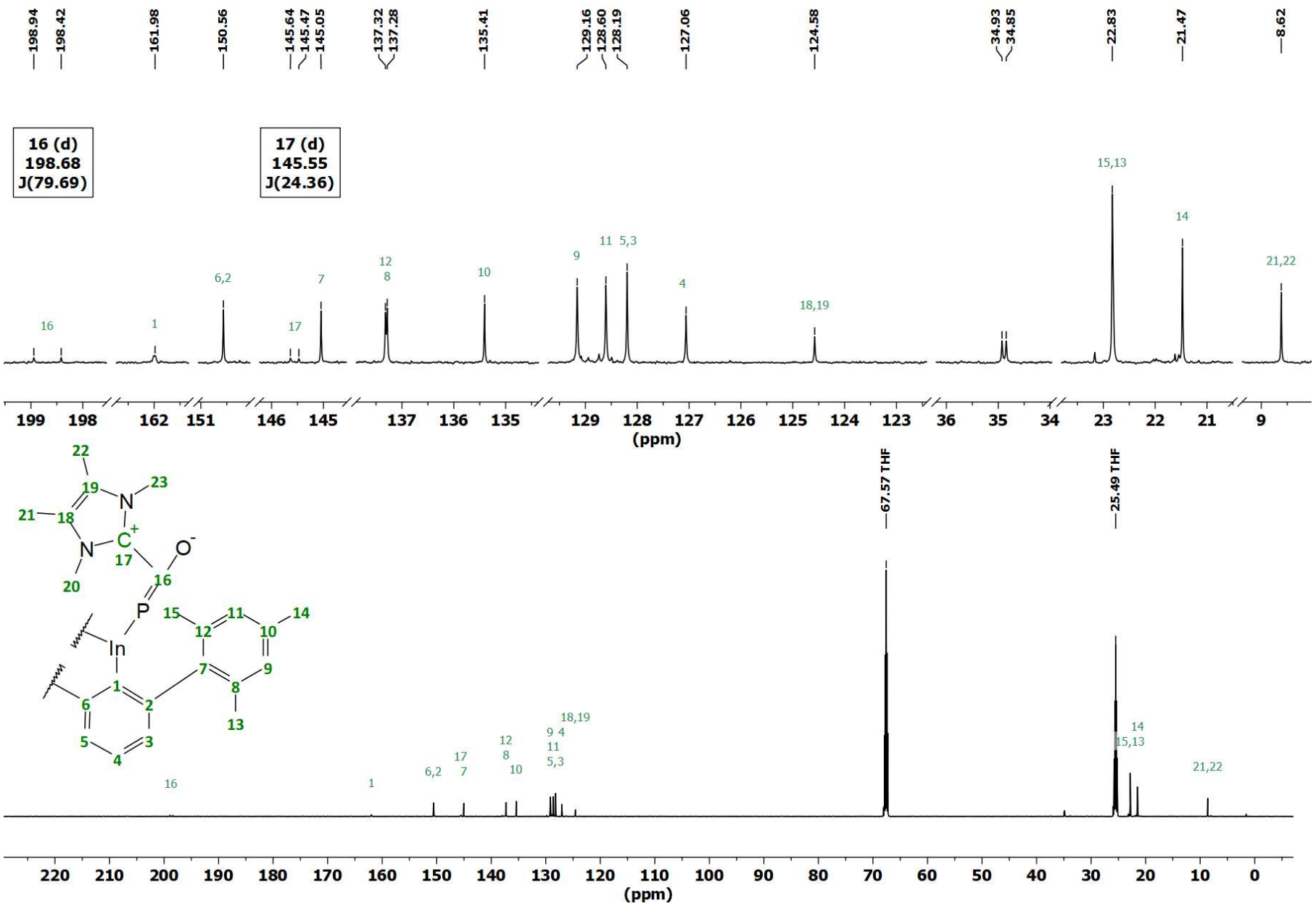

Figure S11. $^{13}C\{^{1}H\}$ NMR (C_6D_6, 151 MHz) spectrum of (2,6-$Mes_2C_6H_3$)$_2$InP(O)C(IMe_4) (**4**).

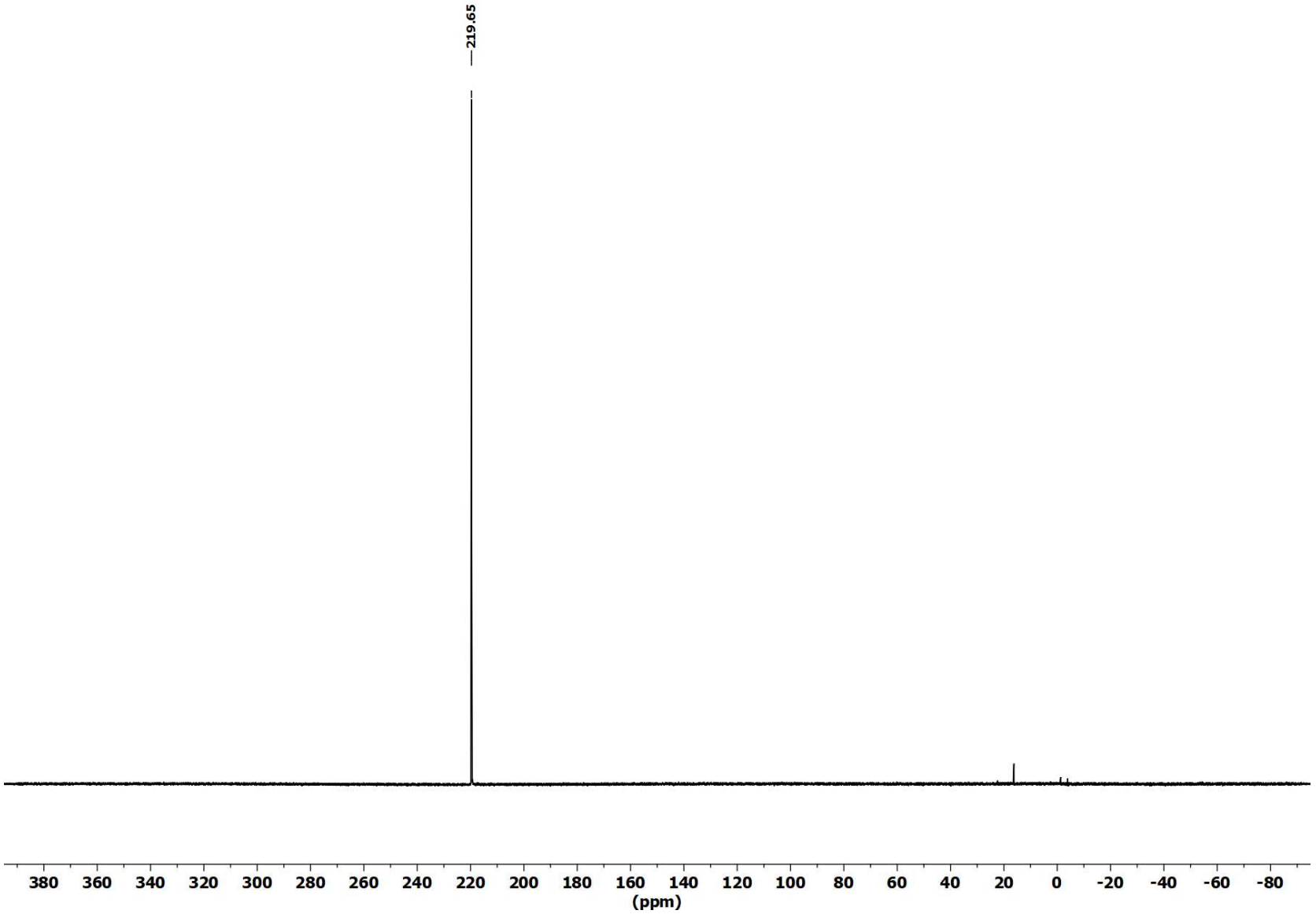

Figure S12. ^{31}P NMR (C_6D_6, 243 MHz) spectrum of (2,6-$Mes_2C_6H_3$)$_2$InP(O)C(IMe_4) (**4**).

Synthesis and characterization of (2,6-Mes$_2$C$_6$H$_3$)$_2$GaTeP(O)C(IMe$_4$) (5)

To a solution of **3** (50.0 mg, 56.8 µmol, 1.00 eq.) in toluene was added an excess of tellurium powder (70.0 mg, 549 µmol, 9.65 Eq.) at room temperature. The resulting suspension was stirred for 18 h. The suspension has been filtered and the solvent of the remaining solution has been removed under reduced pressure to yield **5** as red solid (45.7 mg, 45.3 µmol, 80%).

^{1}H-NMR (600 MHz, THF-d_8): δ (ppm) = 7.10 (t, (t,^3J(^{1}H-^{1}H) = 7.48 Hz, 1H, *p*-C$_6$H$_3$), 7.04 (t, ^3J(^{1}H-^{1}H) = 7.47 Hz, 1H, *p*-C$_6$H$_3$), 6.69 (s (br), 1H, *m*-Mes), 6.68 (s (br), 2H, *m*-Mes), 6.63 (dd, (^3J(^{1}H-^{1}H) = 7.54 Hz, ^4J(^{1}H-^{1}H) = 1.48 Hz, 1H, *m*-C$_6$H$_3$), 6.60 (s (br), 1H, *m*-Mes), 6.57 (s (br), 1H, *m*-Mes), 6.47 (m, 3H, *m*-C$_6$H$_3$), 6.36 (s (br), 1H, *m*-Mes), 6.28 (s (br), 1H, *m*-Mes), 6.24 (s (br), 1H, *m*-Mes), 3.49 (s, 3H), 3.48 (s, 3H), 2.27 (s, 3H), 2.26 (s, 3H), 2.18 (s, 6H), 2.14 (s, 3H), 1.84 (s, 3H), 1.81 (s, 3H), 1.79 (s, 3H), 1.78 (s, 3H), 1.75 (s, 3H),1.73 (s, 3H), 1.62 (s, 3H), 1.44 (s, 3H), 1.26 (s, 3H). **^{13}C{^{1}H}-NMR** (151 MHz, THF-d$_8$): δ(ppm) = 181.75 (d,^1J(^{31}P-^{13}C) = 79.29 Hz, O***C***P), 155.02 (s), 152.15 (s), 151.66 (s), 150.53 (s), 150.42 (s), 149.03 (s), 146.72 (d,^2J(^{31}P-^{13}C) = 40.24 Hz), 145.76 (s), 144.10 (s), 144.07 (s), 139.91 (s), 139.82 (s), 138.33 (s), 138.29 (s), 137.97 (s), 137.46 (s), 137.15 (s), 136.82 (s), 136.53 (s), 136.06 (s), 135.45 (s), 133.53 (s), 131.19 (s, *m*-C$_{Ph}$), 130.75 (s, *m*-C$_{Mes}$), 130.39 (s, *m*-C$_{Ph}$), 130.27 (s, *m*-C$_{Mes}$), 129.72 (s), 129.60 (s, *m*-C$_{Ph}$), 129.40 (s, *m*-C$_{Mes}$), 129.27 (s, *m*-C$_{Mes}$), 129.10 (s, *m*-C$_{Ph}$), 128.96 (s), 128.74 (s, *m*-C$_{Mes}$), 128.59 (s, *m*-C$_{Mes}$), 127.61 (s, *p*-C$_{Ph}$), 127.29 (s, *m*-C$_{Ph}$), 126.73 (s, *m*-C$_{Mes}$), 126.48 (s, *m*-C$_{Mes}$), 125.91 (s), 36.24 (s), 36.14 (s), 24.18 (s), 24.15 (s), 24.06 (s), 23.41 (s), 23.28 (s), 23.23 (s), 22.96 (s), 22.30 (s), 21.26 (s), 21.16 (s), 21.12 (s), 20.93 (s), 8.79 (s). **^{31}P{^{1}H}-NMR** (243MHz, THF-d$_8$): δ(ppm) = 171.86 (^1J(^{125}Te-^{31}P) = 840.09 Hz. **^{125}Te{^{1}H}-NMR** (189MHz, THF-d$_8$): δ(ppm) = –414.42 (d, ^1J(^{125}Te-^{31}P) = 840.09 Hz). **HRMS ESI** (m/z): [M]$^+$ calculated. for C$_{56}$H$_{62}$GaN$_2$OPTe, 1008.29097; found, 1008.29103. **IR** (ATR, neat): $\tilde{\nu}$= 2951 (w), 2915 (m), 2840 (w), 1651 (m), 1609 (w), 1548 (w), 1478 (m), 1432 (s), 1374 (m), 1272 (m), 1221 (w), 1177 (w), 1159 (w), 1113 (w), 1083 (w), 1030 (w), 847 (s), 801 (s), 731 (s), 695 (m) cm^{-1}.

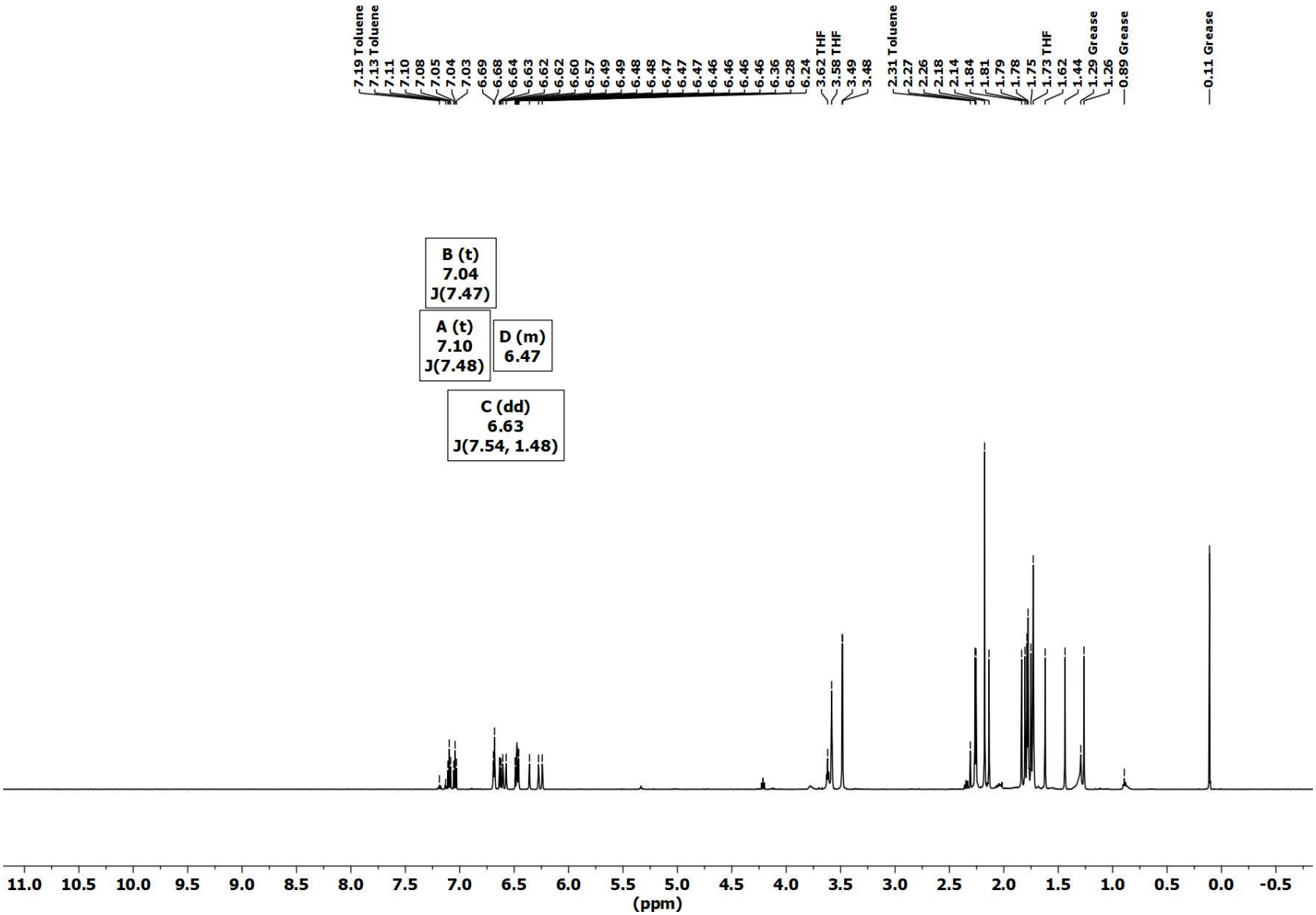

Figure S13. ^{1}H NMR (THF-d$_8$, 600 MHz) spectrum of (2,6-Mes$_2$C$_6$H$_3$)$_2$GaTeP(O)C(IMe$_4$) (**5**).

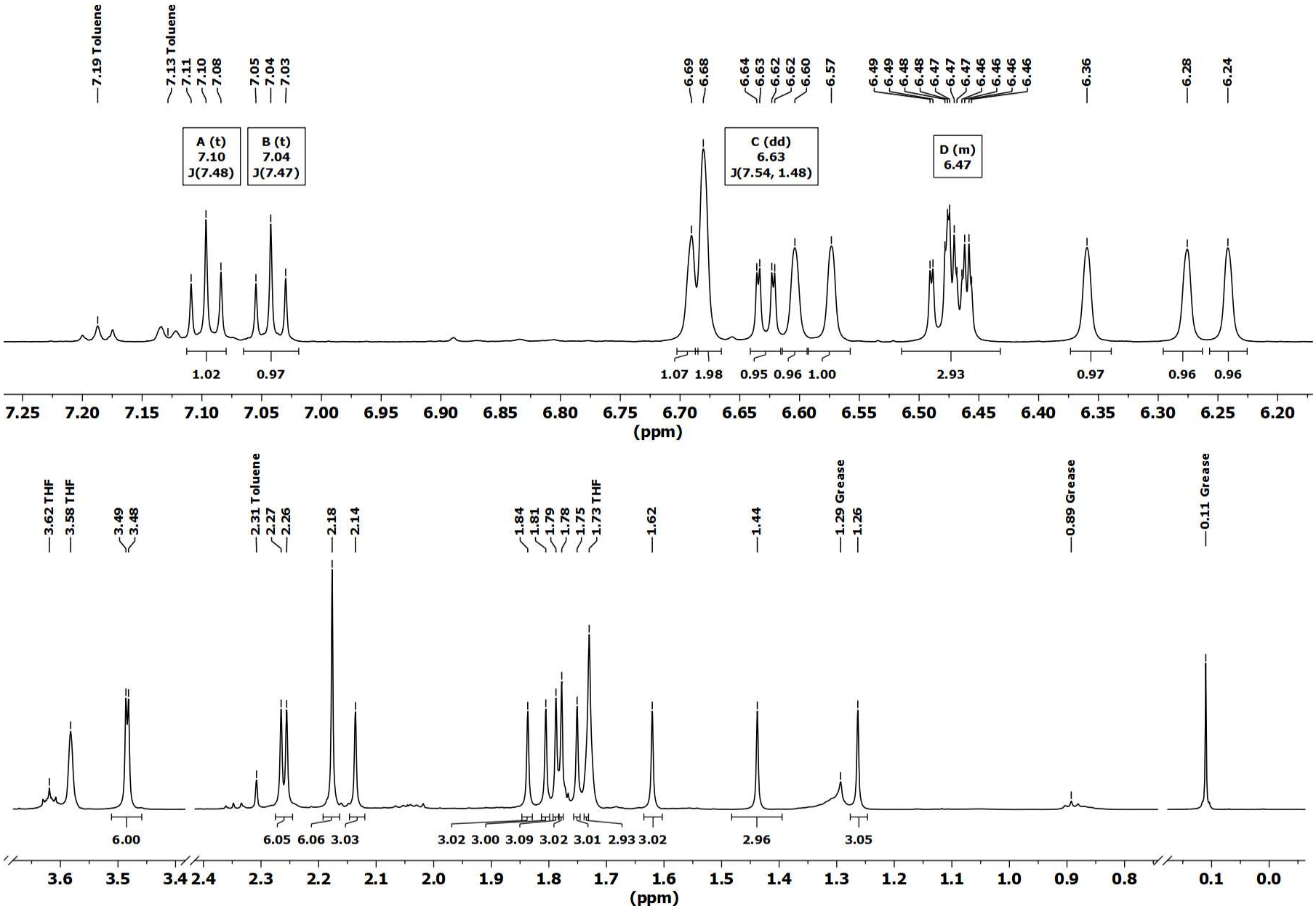

Figure S14. ^{1}H NMR (THF-d8, 600 MHz) zoomed in spectrum of (2,6-$Mes_2C_6H_3$)$_2$GaTeP(O)C(IMe_4) (**5**).

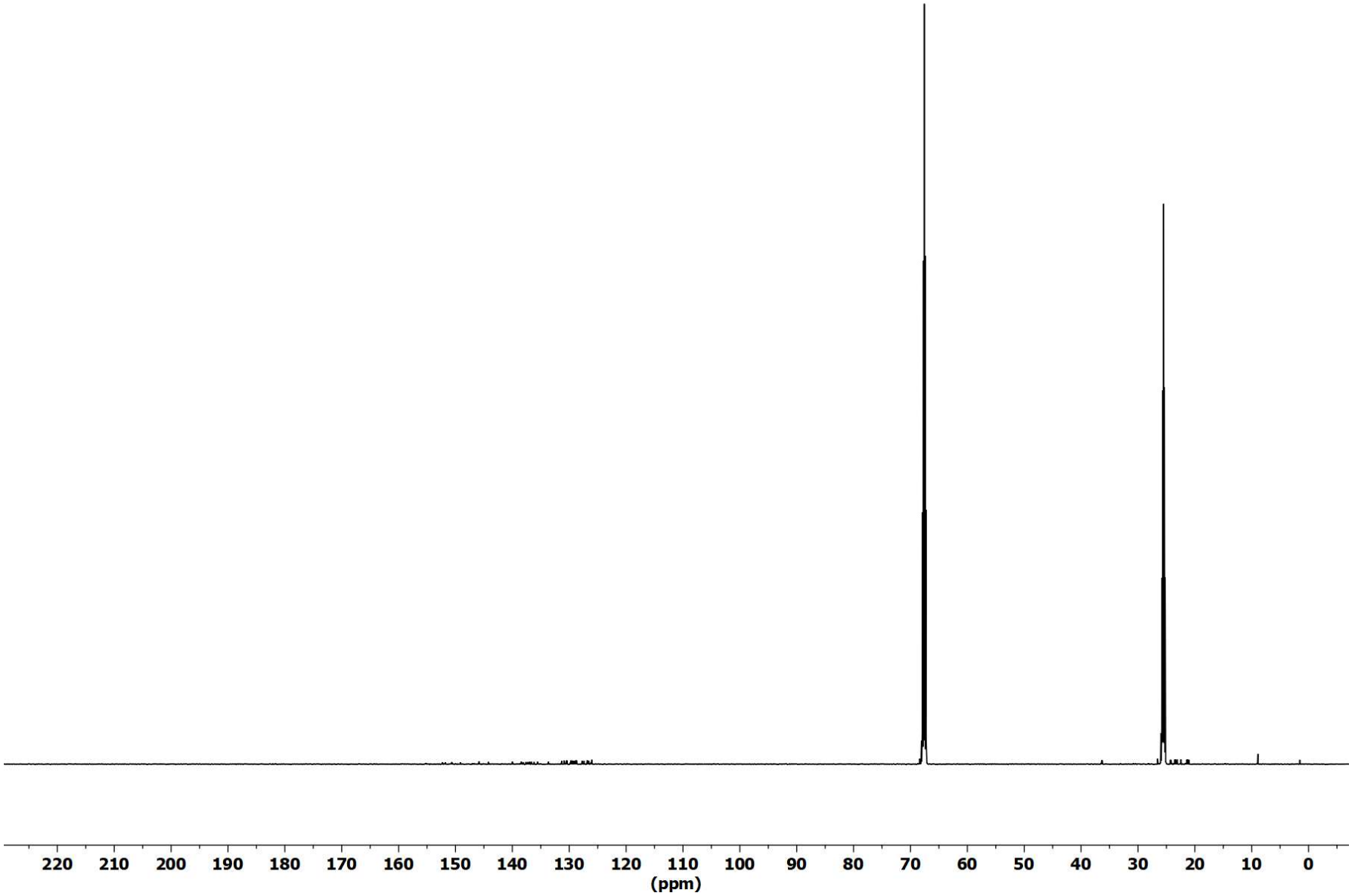

Figure S15. $^{13}C\{^{1}H\}$ NMR (THF-d_8, 151 MHz) spectrum of (2,6-$Mes_2C_6H_3$)$_2$GaTeP(O)C(IMe_4) (**5**).

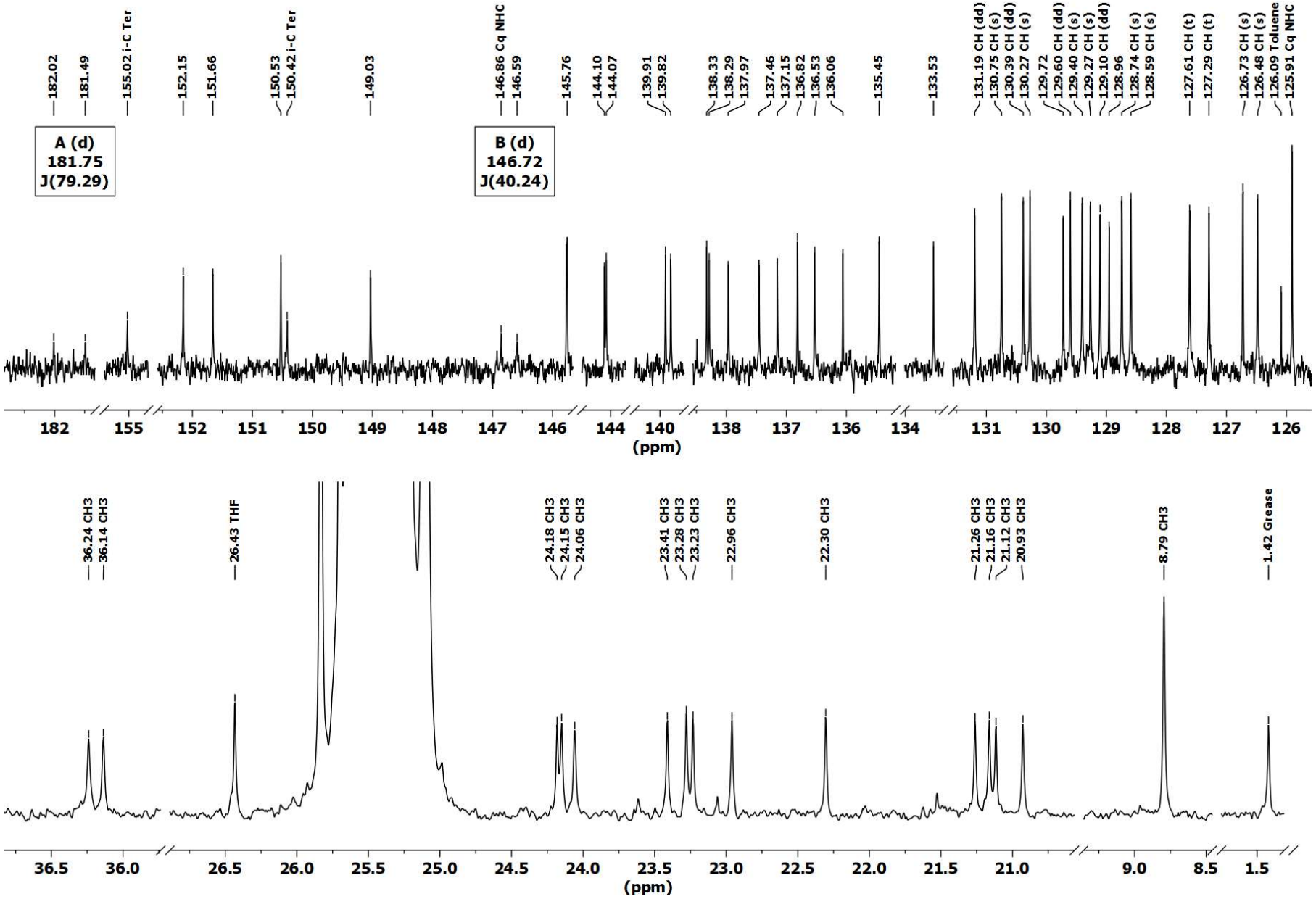

Figure S16. $^{13}C\{^{1}H\}$ NMR (THF-d_8, 151 MHz) zoomed in spectrum of (2,6-$Mes_2C_6H_3$)$_2$GaTeP(O)C(IMe_4) (**5**).

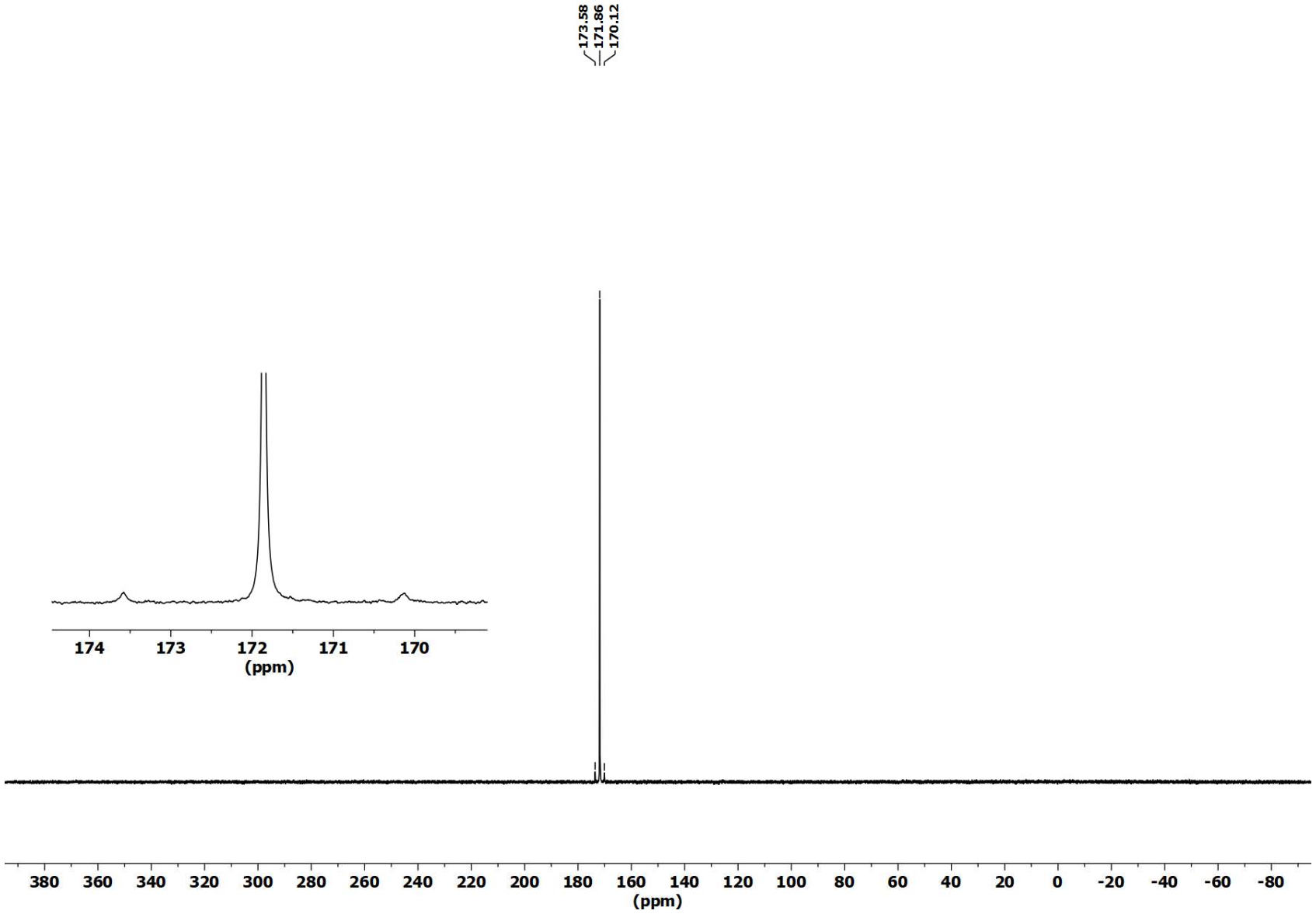

Figure S17. ^{31}P NMR (THF-d_8, 243 MHz) spectrum of (2,6-$Mes_2C_6H_3$)$_2$GaTeP(O)C(IMe_4) (**5**).

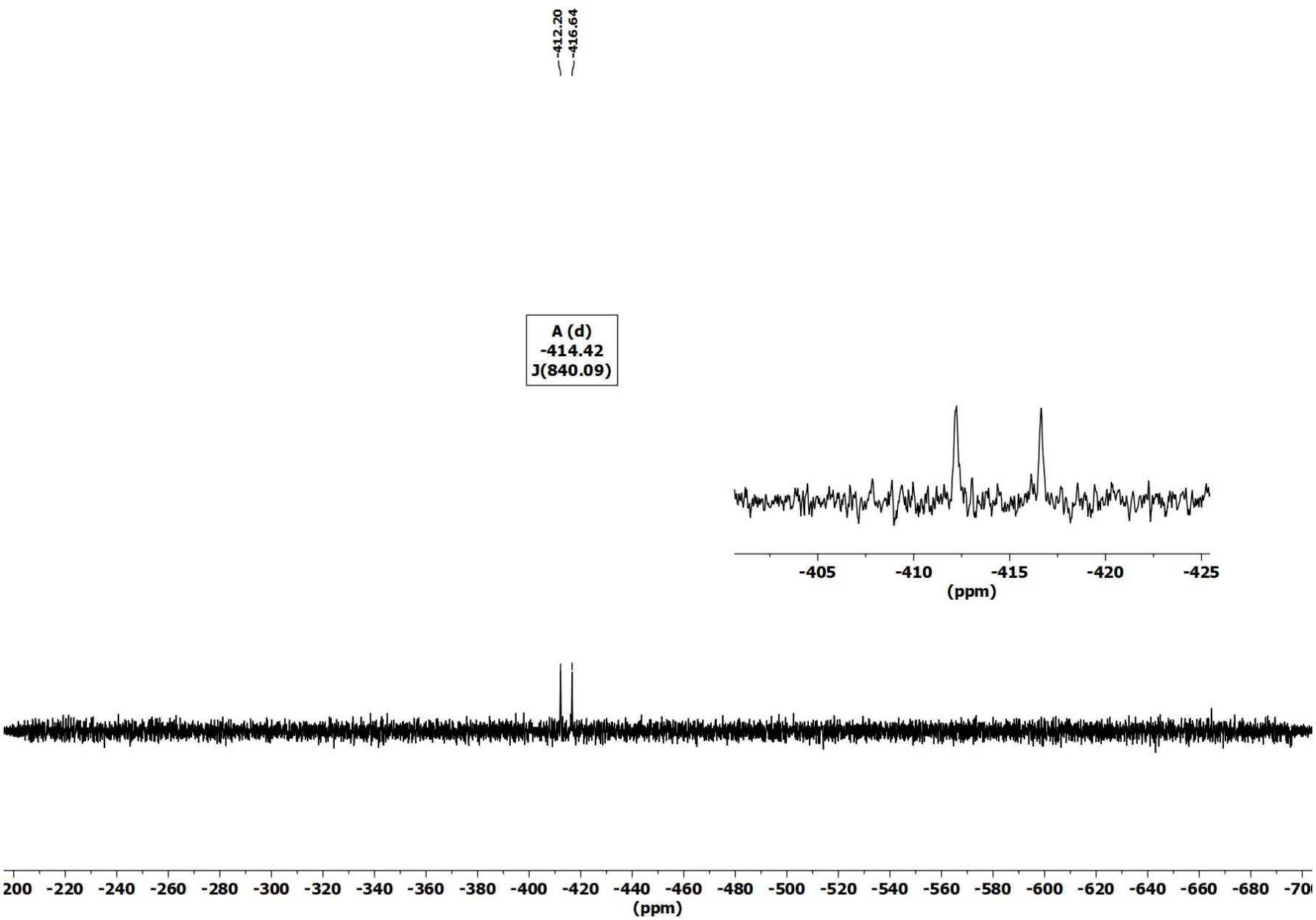

Figure S18. ^{125}Te NMR (THF-d_8, 189 MHz) spectrum of (2,6-$Mes_2C_6H_3$)$_2$GaTeP(O)C(IMe_4) (**5**)

Synthesis and characterization of (2,6-$Mes_2C_6H_3)_2InTeP(O)C(IMe_4)$ (6)

To a solution of **4** (50.0 mg, 56.1 µmol, 1.00 eq.) in toluene was added an excess of tellurium powder (70.0 mg, 549 µmol, 10.0 Eq.) at room temperature. The resulting suspension was stirred for 18 h. The suspension has been filtered and the solvent of the remaining solution has been removed under reduced pressure to yield **6** as orange solid (46.3 mg, 44.0 µmol, 81%).

^{1}H-NMR (600 MHz, THF-d_8) δ (ppm) = 7.06 (t, $^3J(^1H\text{-}^1H)$ = 7.49 Hz, 2H, *p*-C_6H_3), 7.01 (s (br), 1H, *m*-Mes), 6.97 (s (br), 1H, *m*-Mes), 6.80 (s (br), 1H, *m*-Mes), 6.77 (s (br), 1H, *m*-Mes) 6.66 (dd, $^3J(^1H\text{-}^1H)$ = 2.83 Hz, $^4J(^1H\text{-}^1H)$ = 1.42 Hz, 1H, *m*-C_6H_3), 6.65 (dd, $^3J(^1H\text{-}^1H)$ = 2.72 Hz, $^4J(^1H\text{-}^1H)$ = 1.43 Hz, 1H, *m*-C_6H_3), 6.64 (s (br), 1H, *m*-Mes), 6.63 (s (br), 1H, *m*-Mes), 6.59 (s (br), 1H, *m*-Mes), 6.56 (dd, ^3J ($^1H\text{-}^1H$) = 7.58 Hz, ^4J ($^1H\text{-}^1H$) = 1.43 Hz, 1H, *m*-C_6H_3), 6.54 (s (br), 1H, *m*-Mes), 6.53 (dd, ^3J ($^1H\text{-}^1H$) = 7.52 Hz, ^4J ($^1H\text{-}^1H$) = 1.42 Hz, 1H, *m*-C_6H_3), 3.23 (s, 6H), 2.35 (s, 3H), 2.28 (s, 3H), 2.25 (s, 3H), 2.16 (s, 9H), 2.07 (s, 3H), 2x 2.01 (s, 6H), 1.93 (s, 3H), 1.78 (s, 3H), 1.70 (s, 3H), 0.96 (s, 3H), 0.90 (s, 3H).**^{13}C{^{1}H}-NMR** (151 MHz, THF-d_8): δ(ppm) = 198.68 (d,$^1J(^{31}P\text{-}^{13}C)$ = 73.63 Hz, O***C***P), 166.21 (s), 160.23 (s), 151.37 (s), 149.78 (s), 148.97 (s), 148.60 (s) , 148.30 (s), 145.01 (s), 144.73 (s), 143.95 (s), 143.09 (s), 139.47 (s), 139.40 (s), 138.08 (s), 138.05 (s), 137.82 (s), 137.29 (s), 137.05 (s), 136.88 (s), 136.48 (s), 136.42 (s), 135.74 (s), 134.62 (s), 131.29 (s, *m*-C_{Mes}), 130.11 (s, *m*-C_{Mes}), 129.88 (s, *m*-C_{Mes}), 129.37 (s, *m*-C_{Ph}), 129.26 (s, *m*-C_{Ph}), 128.99 (s, *m*-C_{Mes}), 128.76 (s *m*-C_{Mes}), 128.64 (s, *m*-C_{Mes}), 128.50 (s, *m*-C_{Mes}), 128.28 (s, *m*-C_{Ph}), 128.05 (s, *m*-C_{Ph}), 127.57 (s, *p*-C_{Ph}), 127.51 (s, *p*-C_{Ph}), 127.29 (s), 125.62 (s), 33.85 (s), 33.81 (s), 24.35 (s), 24.04 (s), 23.57 (s), 23.14 (s), 22.96 (s), 22.59 (s, *m*-C_{Mes}), 22.54 (s), 21.74 (s), 21.61 (s), 21.54 (s), 21.01 (s), 8.29 (s). **^{31}P{^{1}H}-NMR** (243MHz,THF-d_8): δ(ppm) = 122.26 ($^1J(^{125}Te\text{-}^{31}P)$ = 684.13 Hz). **^{125}Te{^{1}H}-NMR** (189MHz,THF-d_8): δ(ppm) = –544.38 (d, $^1J(^{125}Te\text{-}^{31}P)$ = 682.56 Hz). **HRMS ESI** (m/z): $[M]^+$ calculated. for $C_{56}H_{62}InN_2OPTe$, 1054.27033; found, 1054.26845. **IR** (ATR, neat): $\tilde{\nu}$= 2913 (s), 2851 (m), 1770 (w) 1650 (w), 1610 (w), 1557 (w), 1495 (m), 1433 (s), 1370 (m), 1310 (s), 1228 (w), 1175 (m), 1109 (w), 1078 (w), 1030 (m), 1014 (w), 846 (s), 801 (s), 767 (w), 733 (s), 695 (m), 662 (w) cm^{-1}.

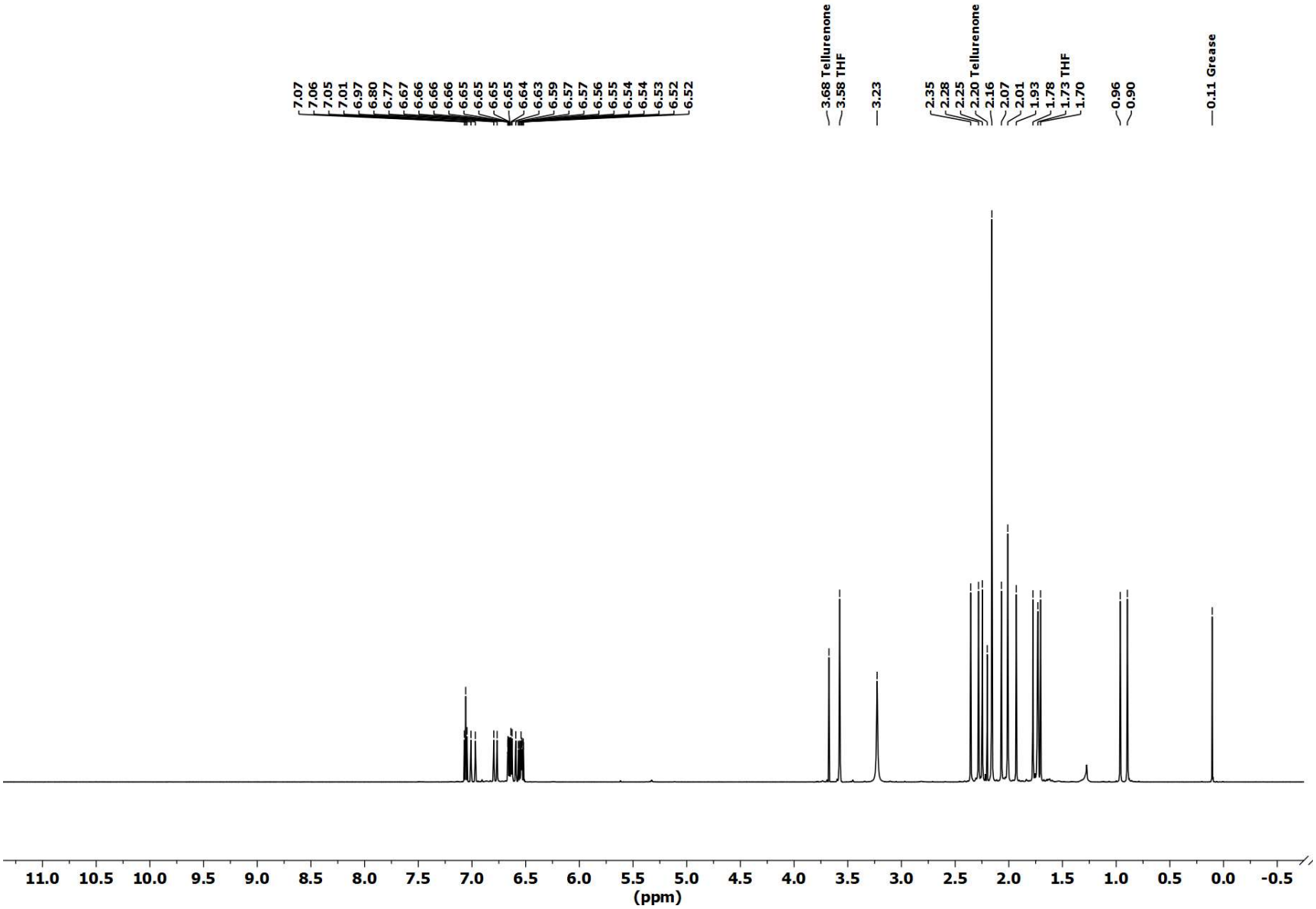

Figure S19. ^{1}H NMR (THF-d_8, 600 MHz) spectrum of (2,6-$Mes_2C_6H_3$)$_2$InTeP(O)C(IMe_4) (**6**).

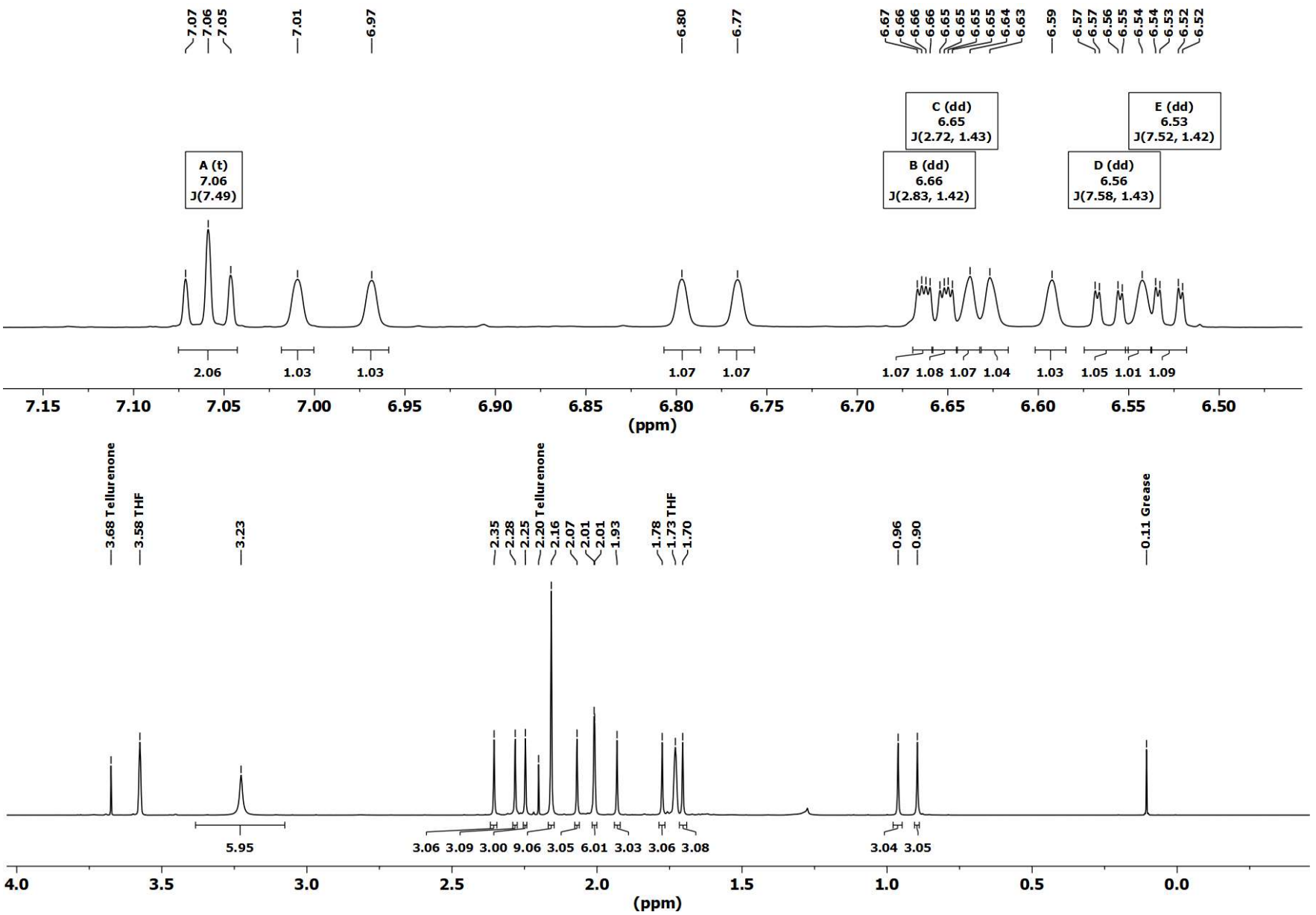

Figure S20. ^{1}H NMR (THF-d_8, 600 MHz) zoomed in spectrum of (2,6-$Mes_2C_6H_3$)$_2$InTeP(O)C(IMe_4) (**6**).

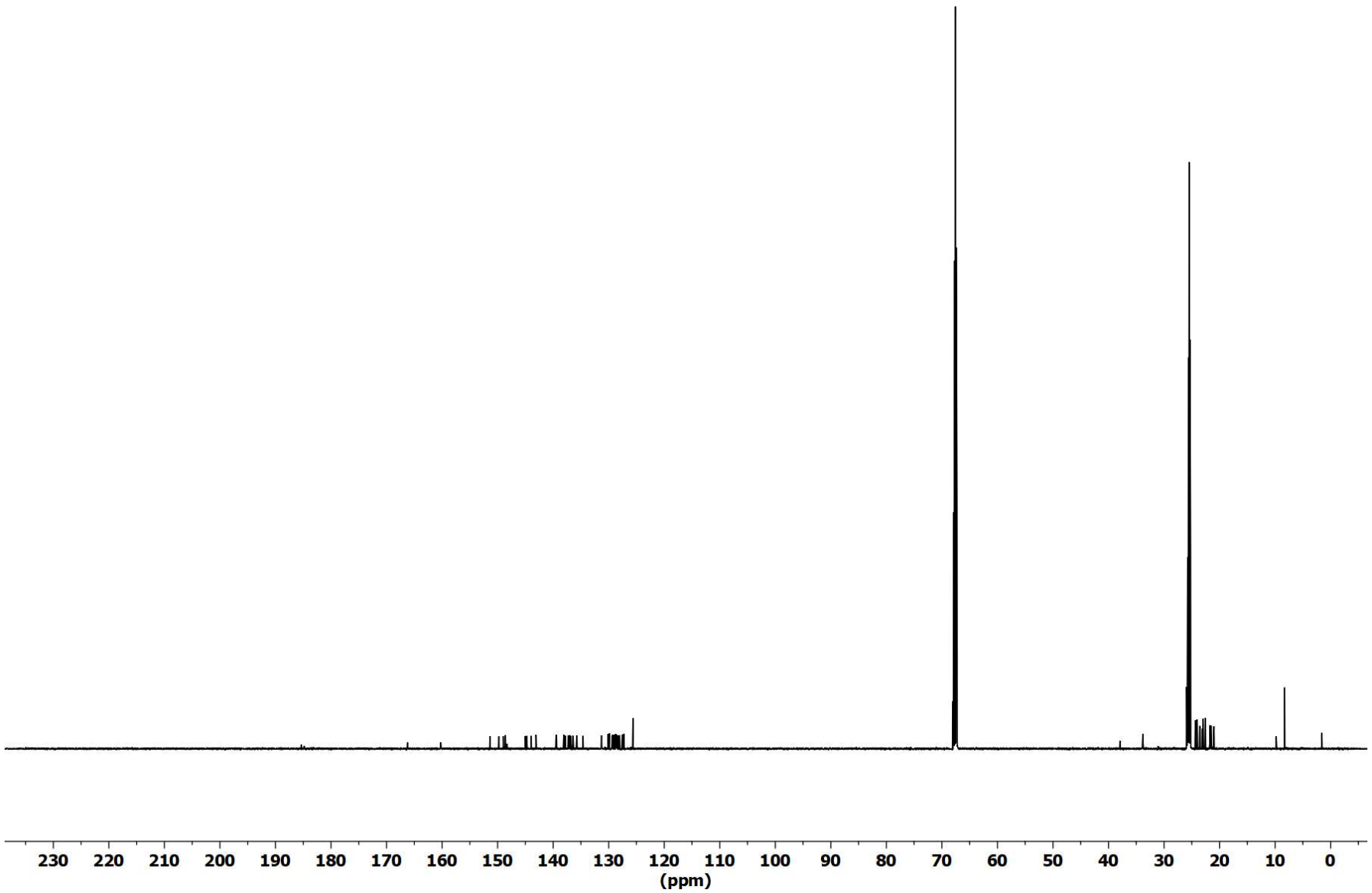

Figure S21. $^{13}C\{^{1}H\}$ NMR (THF-d_8, 151 MHz) spectrum of (2,6-$Mes_2C_6H_3$)$_2$InTeP(O)C(IMe_4) (**6**).

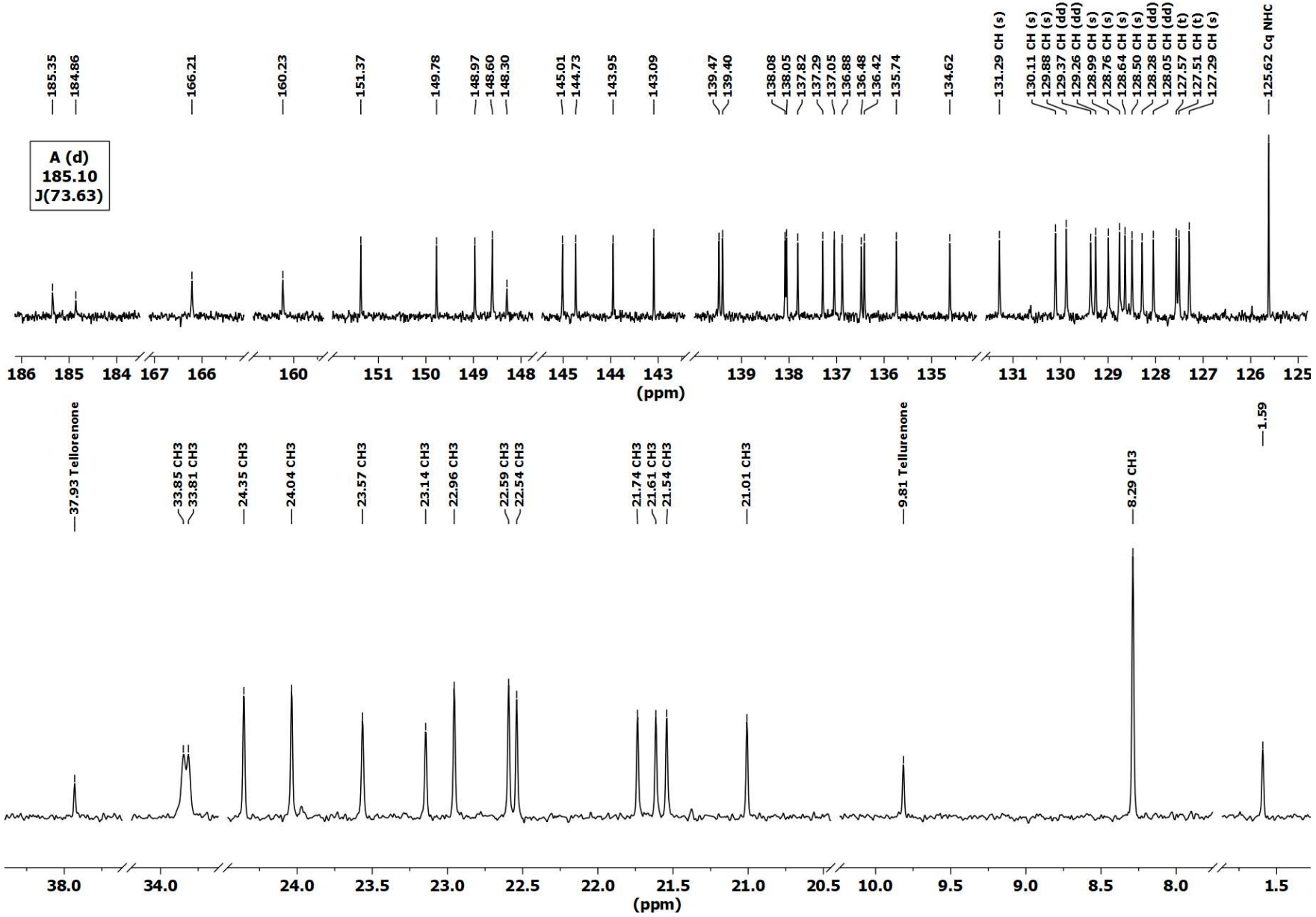

Figure S22. $^{13}C\{^{1}H\}$ NMR (THF-d_8, 151 MHz) zoomed in spectrum of (2,6-$Mes_2C_6H_3$)$_2$InTeP(O)C(IMe_4) (**6**).

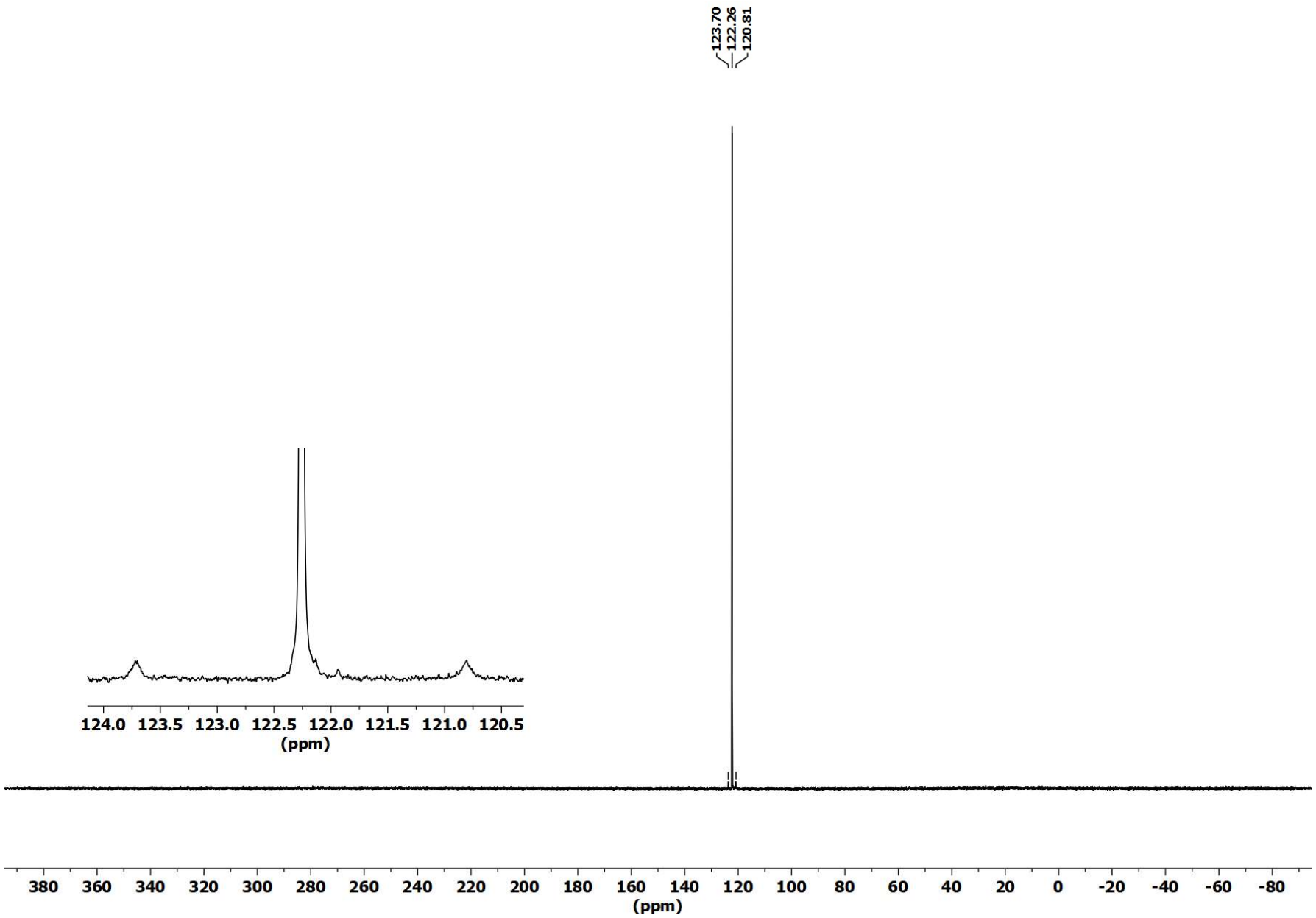

Figure S23. ^{31}P NMR (THF-d_8, 243 MHz) spectrum of (2,6-$Mes_2C_6H_3$)$_2$InTeP(O)C(IMe_4) (**6**)

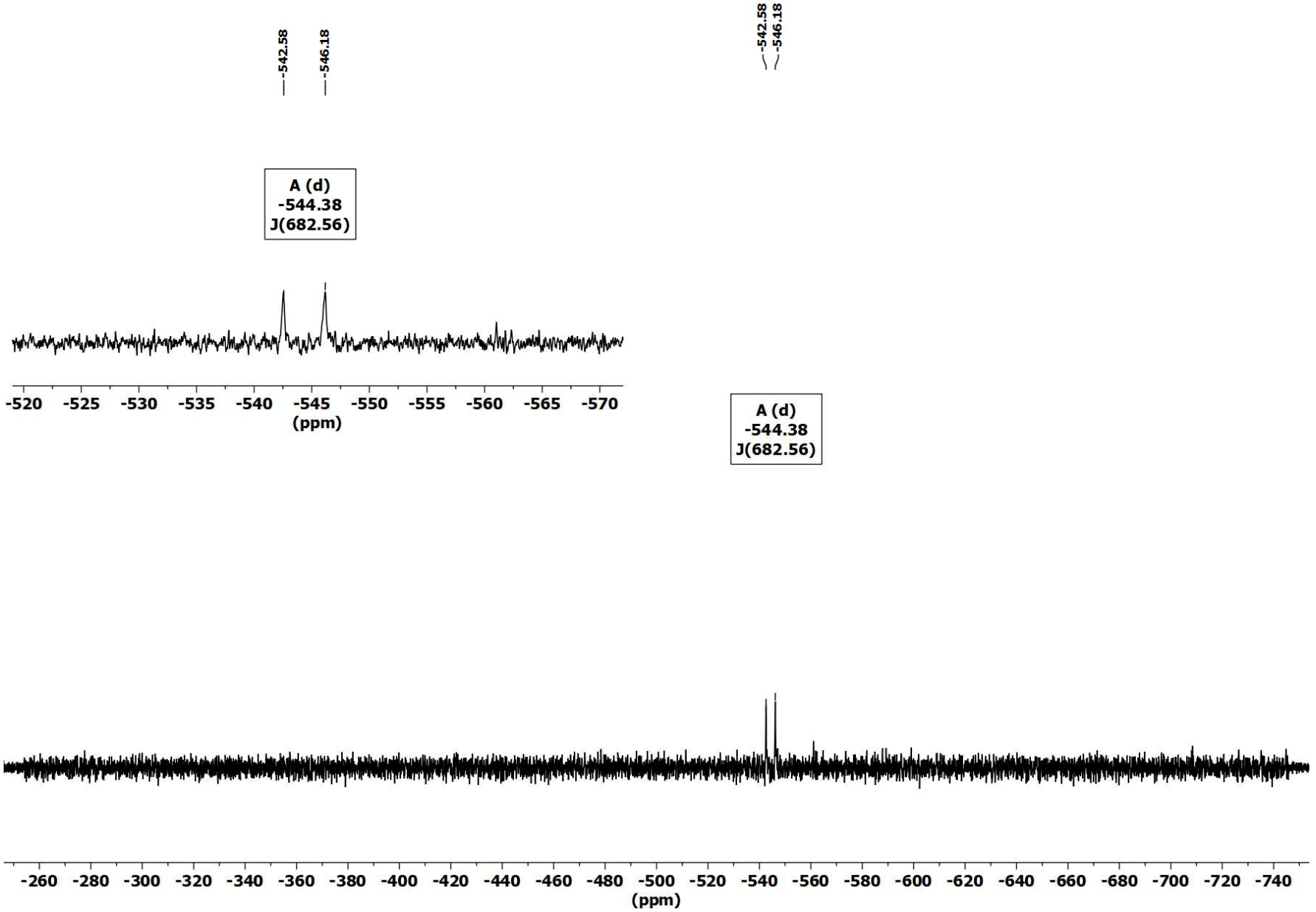

Figure S24. ^{125}Te NMR (THF-d_8, 189 MHz) spectrum of (2,6-$Mes_2C_6H_3$)$_2$InTeP(O)C(IMe_4) (**6**).

X-Ray diffraction studies

Single crystals suitable for X-Ray structure determination were grown from hot toluene solutions (**1**, **2**, **4**, **5** and **6**·toluene) or by diffusion of *n*-hexane into a CH_2Cl_2 solutions (**3**). Intensity data were collected on a Bruker Venture D8 diffractometer at 100 K with graphite-monochromated Mo-Kα (0.7107 Å) radiation. All structures were solved by direct methods and refined based on F^2 by use of the SHELX program package as implemented in Olex2.[S5] All non-hydrogen atoms were refined using anisotropic displacement parameters. Hydrogen atoms attached to carbon atoms were included in geometrically calculated positions using a riding model. Crystal and refinement data are collected in Table S1. Figures were created using DIAMOND.[S6]

Table S1. Crystal data and structure refinement of **1-6.**

	1	**2**	**3**
Formula	$C_{49}H_{50}GaOP$	$C_{49}H_{50}InOP$	$C_{56}H_{62}GaN_2OP$
Formula weight, g mol^{-1}	755.58	800.68	879.76
Crystal system	Triclinic	triclinic	monoclinic
Crystal size, mm	0.24 × 0.13 × 0.12	0.21 × 0.12 × 0.07	0.18 × 0.15 × 0.09
Space group	$P\bar{1}$	$P\bar{1}$	$P2_1/n$
a, Å	10.4559(7)	10.6724(3)	11.0545(12)
b, Å	11.2875(7)	11.2002(4)	19.948(2)
c, Å	16.7900(10)	16.8476(5)	22.110(2)
α, º	88.711(2)	88.6950(10)	90
β, º	81.094(3)	80.3120(10)	98.272(3)
γ, º	82.517(3)	81.7330(10)	90
V, Å^3	1941.0(2)	1964.49(11)	4824.7(9)
Z	2	2	4
ρ_{calcd}, Mg m^{-3}	1.293	1.354	1.211
μ (Mo $K\alpha$), mm^{-1}	0.787	0.679	0.644
F(000)	796	832	1864
θ range, deg	2.17 to 36.38	2.21 to 33.28	2.12 to 25.00
Index ranges	–13 ≤ h ≤ 13	–16 ≤ h ≤ 16	–11 ≤ h ≤ 13
	–14 ≤ k ≤ 14	–17 ≤ k ≤ 17	–23 ≤ k ≤ 23
	–22 ≤ l ≤ 22	–25 ≤ l ≤ 25	–26 ≤ l ≤ 26
No. of reflns collected	51824	122752	27261
Completeness to θ_{max}	99.6%	99.9%	99.8%
No. indep. Reflns	9335	15094	8489
No. obsd reflns with($I>2\sigma(I)$)	7836	13210	6300
No. refined params	481	481	542
GooF (F^2)	1.074	1.039	1.101
R_1 (F) ($I > 2\sigma(I)$)	0.0518	0.0283	0.0803
wR_2 (F^2) (all data)	0.1335	0.0657	0.1585
Largest diff peak/hole, e Å^{-3}	1.709 / –1.543	0.686 / –0.477	1.206 / –1.149
CCDC number	2105254	2105255	2105256

Table S1. Cont.

4	**5**	**6**·toluene
$C_{56}H_{62}InN_2OP$	$C_{56}H_{62}GaN_2OPTe$	$C_{63}H_{70}InN_2OPTe$
924.86	1007.36	1144.60
monoclinic	monoclinic	monoclinic
0.32 × 0.23 × 0.16	0.47 × 0.15 × 0.11	0.25 × 0.20 × 0.14
$P2_1/n$	$P2_1/n$	$P2_1/n$
11.2294(5)	11.6850(8)	11.4267(10)
20.1471(12)	33.106(2)	28.438(3)
22.3970(12)	13.6771(12)	17.4895(14)
90	90	90
100.753(2)	110.903(2)	104.738(3)
90	90	90
4978.1(5)	4942.7(7)	5496.3(9)
4	4	4
1.234	1.354	1.383
0.546	1.208	1.022
1936	2072	2344
1.98 to 28.46	2.33 to 28.28	1.98 to 33.26
–13 ≤ h ≤ 13	–15 ≤ h ≤ 15	–13 ≤ h ≤ 17
–24 ≤ k ≤ 24	–44 ≤ k ≤ 44	–43 ≤ k ≤ 43
–27 ≤ l ≤ 27	–18 ≤ l ≤ 18	–26 ≤ l ≤ 26
91075	113392	95732
99.9%	99.8%	99.8%
9791	12243	21074
8776	10846	14438
582	575	575
1.294	1.178	1.022
0.0679	0.0521	0.0496
0.1345	0.1183	0.0842
0.674 / –1.362	1.121 / –1.843	0.717 / –0.629
2105257	2105258	2105259

Computational methodology

Density functional theory (DFT) computations were performed in the gas-phase at the B3PW91/6-311+G(2df,p)[S7] level of theory using Gaussian09.[S8] For the In, Tl and Te atoms, effective core potentials (ECP28MDF, ECP60MDF)[S9] and corresponding cc-pVTZ basis set[S9] were utilized. Dispersion was taken account for by the empirical dispersion correction of Grimme.[S10] Subsequent normal mode analysis had to be skipped as it exceeded computational capacities. The wavefunction files were used for a topological analysis of the electron density according to the Atoms-In-Molecules space-partitioning scheme[16] using AIM2000,[S11] whereas DGRID[S12] was used to generate and analyze the Electron-Localizability-Indicator (ELI-D)[18] related real-space bonding descriptors applying a grid step size of 0.05 a.u. (0.12 a.u. for visualization). The NCI[17] grids were computed with NCIplot (0.1 a.u. grids).[S13] Bond paths are displayed with AIM2000, ELI-D and NCI figures are displayed with MolIso,[S14] and spin densities are displayed with GaussView. AIM provides a bond paths motif, which resembles and exceeds the Lewis picture of chemical bonding, disclosing all types and strengths of interactions. Additionally, it provides atomic volumes and charges. Analyses of the reduced density gradient, $s(\mathbf{r}) = [1/2(3\pi^2)^{1/3}]|\nabla\rho|/\rho^{4/3}$, according to the NCI method is used to visualize non-covalent bonding aspects. An estimation of different non-covalent contact types according to steric/repulsive ($\lambda_2 > 0$), van der Waals-like ($\lambda_2 \approx 0$), and attractive ($\lambda_2 < 0$) is facilitated by mapping the ED times the sign of the second eigenvalue of the Hessian ($\text{sign}(\lambda_2)\rho$) on the *iso*-surfaces of $s(\mathbf{r})$. AIM and NCI are complemented by the ELI-D, which provides electron populations and volumes of bonding and lone-pair basins and is especially suitable for the analysis of (polar-)covalent bonding aspects.

Table S2. Calculated bond lengths and relative energies of (2,6-$Mes_2C_6H_3)_2$EPCO and (2,6-$Mes_2C_6H_3)_2$EOCP (E = B, Al, Ga, In, Tl).

Coord. mode	energy	delta	kJ mol^{-1}	d(E-P)	d(E-C)	d(E-O)	d(P-C)	d(C-O)
B-P-C-O	–2338.8817	–0.0029	–7.70	1.903	2.727	3.716	1.676	1.151
B-O-C-P	–2338.8788			3.951	2.457	1.390	1.546	1.275
Al-P-C-O	–2556.5002	–0.0086	–22.65	2.356	2.728	3.509	1.645	1.166
Al-O-C-P	–2556.4916			4.541	2.982	1.738	1.559	1.244
Ga-P-C-O	–4238.9190	–0.0202	–53.03	2.375	2.788	3.579	1.645	1.165
Ga-O-C-P	–4238.8988			4.236	2.830	1.922	1.565	1.249
In-P-C-O	–2504.3252	–0.0250	–65.53	2.579	2.950	3.708	1.641	1.169
In-O-C-P	–2504.3002			4.367	3.013	2.183	1.574	1.238
Tl-P-C-O	–2486.6805	–0.0234	–61.34	2.683	3.030	3.759	1.637	1.173
Tl-O-C-P	–2486.6571			4.453	3.141	2.374	1.583	1.226

Table S3. Dissociation of (2,6-$Mes_2C_6H_3)_2$EPCO into [(2,6-$Mes_2C_6H_3)_2$E]$^+$ and [PCO]$^-$.

E	[(2,6-$Mes_2C_6H_3)_2$E]$^+$	[(2,6-$Mes_2C_6H_3)_2$E]PCO	delta	kJ mol^{-1}
[PCO]$^-$	–454.6960			
B	–1884.0135	–2338.7095	–0.1722	–452.2
Al	–2101.6276	–2556.3236	–0.1766	–463.7
Ga	–3784.0489	–4238.7449	–0.1741	–457.2
In	–2049.4587	–2504.1546	–0.1705	–447.7
Tl	–2031.8282	–2486.5242	–0.1563	–410.5

Table S4. Calculated bond lengths and dissociation of (2,6-$Mes_2C_6H_3)_2$EP(O)C(IMe_4) into (2,6-$Mes_2C_6H_3)_2$EPCO and IMe_4 (E = B, Al, Ga, In, Tl).

E	energy	delta	kJ mol^{-1}	d(E-P)	d(E-C)	d(E-O)	d(P-C)	d(C-O)
IMe_4	-383.4438							
B	-2722.3925	-0.067	-175.7	2.074	2.149	1.555	1.709	1.344
Al	-2940.0211	-0.077	-202.3	2.411	2.377	1.862	1.720	1.334
Ga	-4622.4235	-0.061	-159.2	2.416	2.496	2.032	1.724	1.316
In	-2887.8199	-0.051	-133.6	2.592	2.707	2.281	1.730	1.303
Tl	-2870.1656	-0.041	-108.4	2.642	2.841	2.513	1.735	1.284

Table S5. Calculated bond lengths of (2,6-$Mes_2C_6H_3)_2$ETeP(O)C(IMe_4)

E	d(E-P)	d(E-C)	d(E-O)	d(P-C)	d(C-O)	d(E-Te)
Ga	3.622	2.933	1.964	1.721	1.304	2.689
In	3.800	3.146	2.203	1.728	1.292	2.842

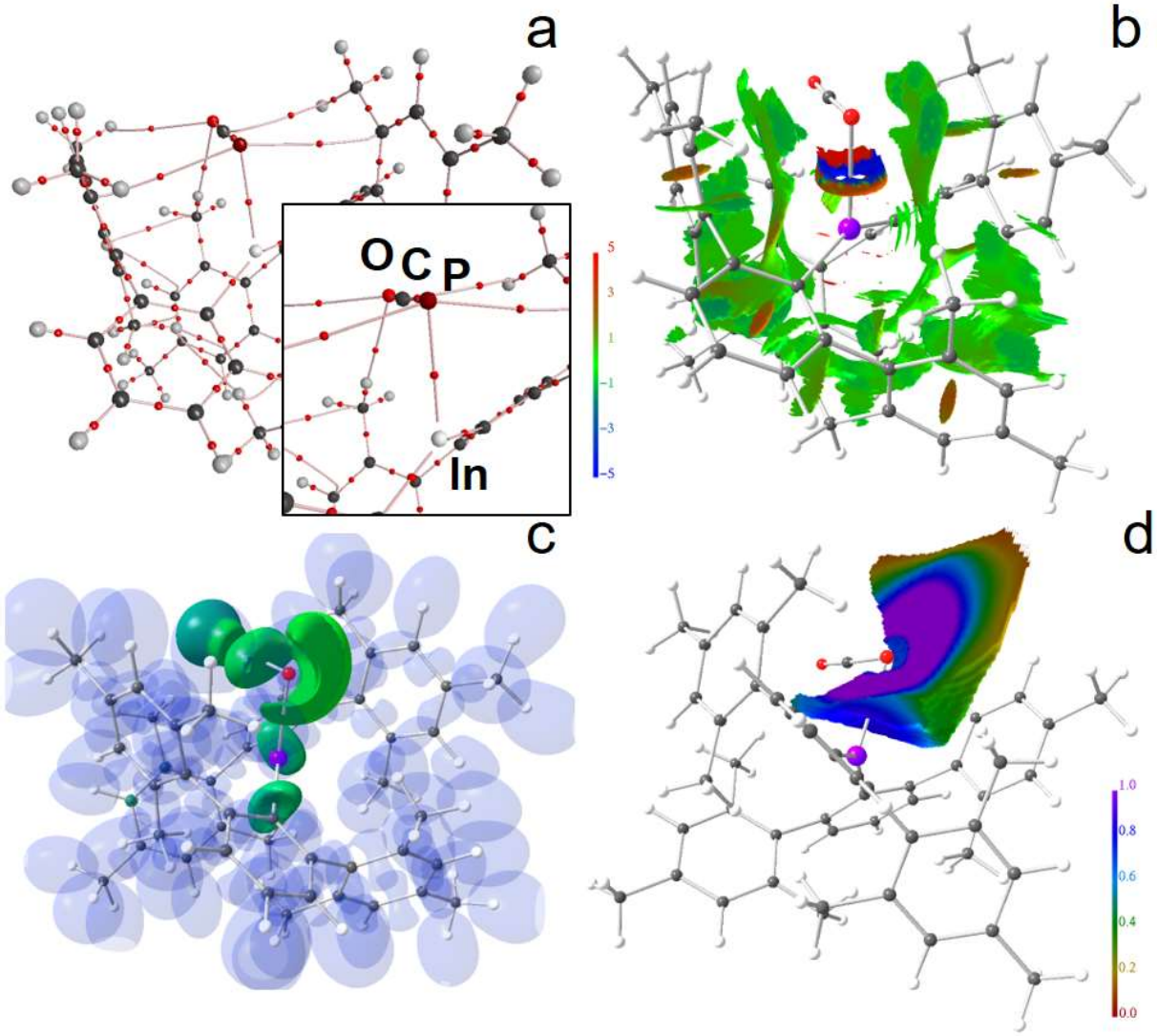

Figure S25. RSBI analysis of **2** (a) AIM bond paths motif, (b) NCI *iso*-surface at s(r) = 0.5, (c) ELI-D localization domain representation at *iso*-value of 1.3, (d) ELI-D distribution mapped on the In-P ELI-D basin.

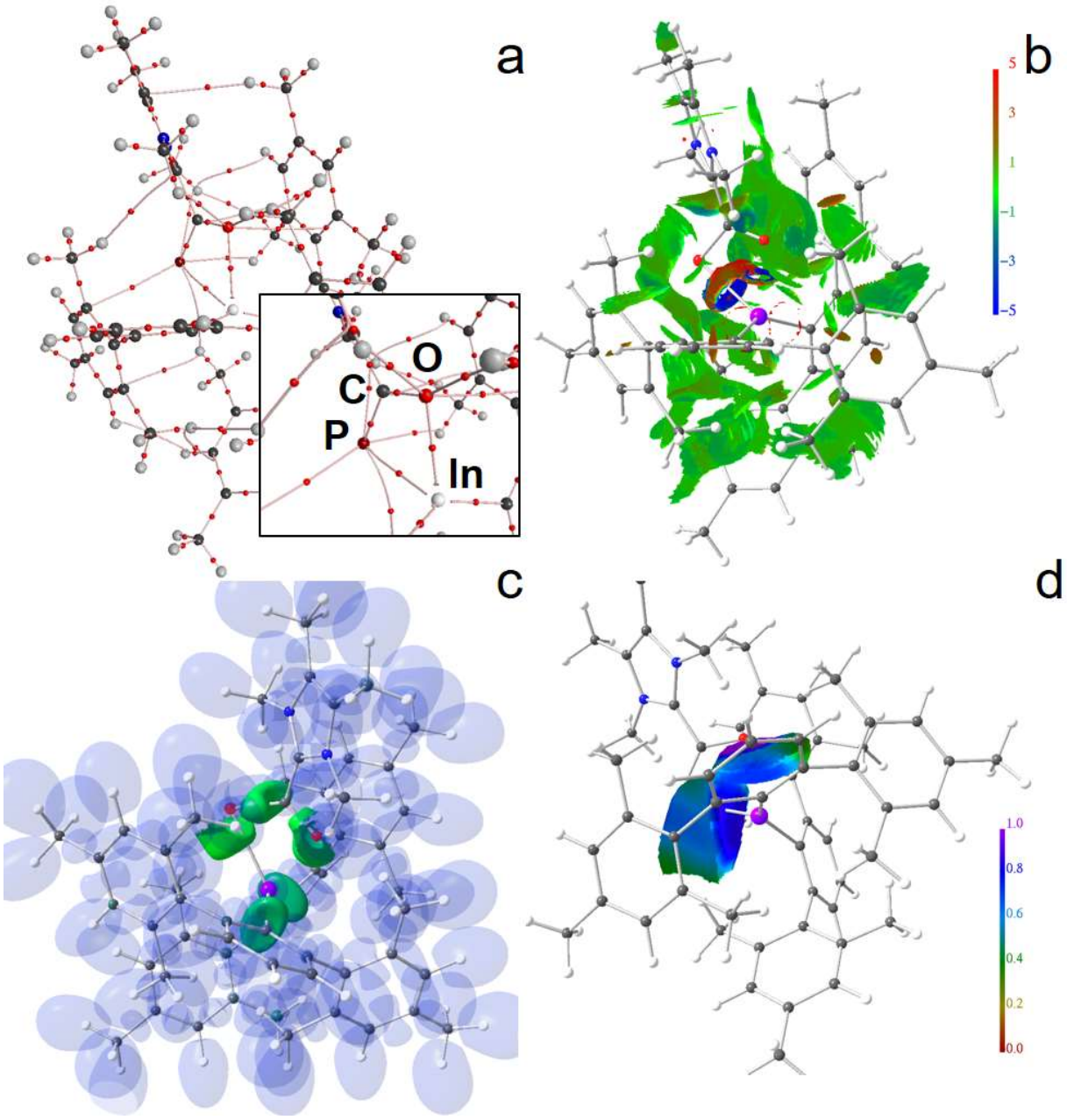

Figure S26. RSBI analysis of **4** (a) AIM bond paths motif, (b) NCI *iso*-surface at s(r) = 0.5, (c) ELI-D localization domain representation at *iso*-value of 1.3, (d) ELI-D distribution mapped on the In-P and In-O ELI-D basins.

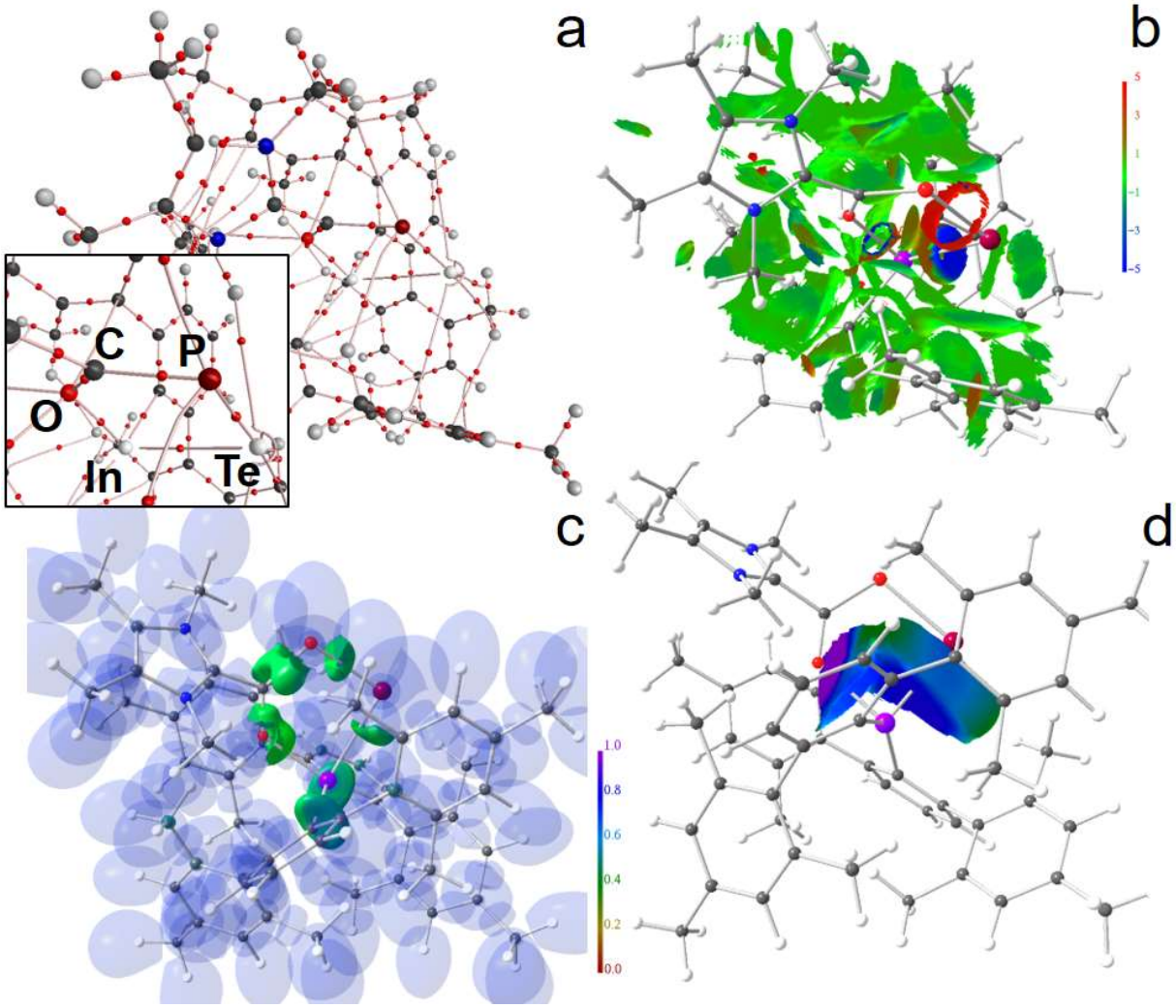

Figure S27. RSBI analysis of **6** (a) AIM bond paths motif, (b) NCI *iso*-surface at s(r) = 0.5, (c) ELI-D localization domain representation at *iso*-value of 1.3, (d) ELI-D distribution mapped on the In-O and In-Te ELI-D basins.

References

[S1] X.-W. Li, W. T. Pennington, G. H. Robinson, *Organometallics* **1995**, *14*, 2109-2111.

[S2] X.-W. Li, G. Robinson, W. T. Pennington, *Main Group Chem*. 1996, *1*, 301-307.

[S3] R. E. Schreiber, J. M. Goicoecha, *Angew. Chem. Int. Ed*. **2021**, *60*, 3759-3767.

[S4] A. J. Arduengo III, H. V. R. Dias, R. L. Harlow, M. Kline, *J. Am. Chem. Soc*. **1992**, *114*, 5530-5534.

[S5] O. V. Dolomanov, L. J. Bourhis, R. J. Gildea, J. A. K. Howard, H. Puschmann. *J. Appl. Cryst.* **2009**, *42*, 339–341.

[S6] K. Brandenburg, H. Putz, Crystal Impact GbR, Bonn **2012**.

[S7] (a) A. D. Becke, *J. Chem. Phys*. **1993**, *98*, 5648-5652. (b) J. P. Perdew, J. A. Chevary, S. H. Vosko, K. A. Jackson, M. R. Pederson, D. J. Singh, C. Fiolhais, *Phys. Rev*. B **1992**, *46*, 6671-6687.

[S8] Gaussian 16, Revision C.01, M. J. Frisch, G. W. Trucks, H. B. Schlegel, G. E. Scuseria, M. A. Robb, J. R. Cheeseman, G. Scalmani, V. Barone, G. A. Petersson, H. Nakatsuji, X. Li, M. Caricato, A. V. Marenich, J. Bloino, B. G. Janesko, R. Gomperts, B. Mennucci, H. P. Hratchian, J. V. Ortiz, A. F. Izmaylov, J. L. Sonnenberg, D. Williams-Young, F. Ding, F. Lipparini, F. Egidi, J. Goings, B. Peng, A. Petrone, T. Henderson, D. Ranasinghe, V. G. Zakrzewski, J. Gao, N. Rega, G. Zheng, W. Liang, M Hada, M. Ehara, K. Toyota, R. Fukuda, J. Hasegawa, M. Ishida, T. Nakajima, Y. Honda, O. Kitao, H. Nakai, T. Vreven, K. Throssell, J. A. Jr. Montgomery, J. E. Peralta, F. Ogliaro, M. J. Bearpark, J. J. Heyd, E. N. Brothers, K. N. Kudin, V. N. Staroverov, T. A. Keith, R. Kobayashi, J. Normand, K. Raghavachari, A. P. Rendell, J. C. Burant, S. S. Iyengar, J. Tomasi, M. Cossi, J. M. Millam, M. Klene, C. Adamo, R. Cammi, J. W. Ochterski, R. L. Martin, K. Morokuma, O. Farkas, J. B. Foresman, D. J. Fox, Gaussian, Inc., Wallingford CT, 2016.

[S9] K. A. Peterson, *J. Chem. Phys.* **2003**, *119*, 11099.

[S10] S. Grimme, J. Anthony, S. Ehrlich, H. Krieg, *J. Chem. Phys*. **2010**, *132*, 154104.

[S11] F. Biegler-König, J. Schönbohm, D. Bayles, *J. Comput. Chem*. **2001**, *22*, 545-559.

[S12] M. Kohout, *DGRID*-4.6 Radebeul, **2015**.

[S13] J. Contreras-García, E. Johnson, S. Keinan, R. Chaudret, J.-P. Piquemal, D. Beratan, W. Yang, *J. Chem. Theor. Comp.* **2011**, *7*, 625-632.

[S14] C. B. Hübschle, P. Luger, *J. Appl. Crystallogr*. **2006**, *39*, 901-904.